2mw4

NASA TECHNICAL TRANSLATION TT F-15,114

ELASTIC VIBRATIONS IN ROLLER BEARINGS I. THE ROTATING MASS IS BALANCED WITH RESPECT TO ITS OWN ROTATIONAL AXIS

B. Szoke

Translation of: "Acta Technica Academiae Scientiarum Hungaricae", Volume 72, Nos. 1-2, 1972, pp. 3-72.

(NASA-TT-F-15114) ELASTIC VIBRATIONS IN ROLLER BEARINGS. 1: THE ROTATING MASS IS BALANCED WITH RESPECT TO ITS OWN ROTATIONAL AXIS (Techtran Corp.) ~~70~~ p HC $5.50 68 CSCL 13I G3/15

N74-12234

Unclas 23318

NATIONAL AERONAUTICS AND SPACE ADMINISTRATION
WASHINGTON, D. C. 20546 NOVEMBER 1973

STANDARD TITLE PAGE

1. Report No. NASA TT F-15,114	2. Government Accession No.	3. Recipient's Catalog No.
4. Title and Subtitle ELASTIC VIBRATIONS IN ROLLER BEARINGS. I. THE ROTATING MASS IS BALANCED WITH RESPECT TO ITS OWN ROTATIONAL AXIS		5. Report Date 6. Performing Organization Code
7. Author(s) B. Szoke		8. Performing Organization Report No. 10. Work Unit No.
9. Performing Organization Name and Address Techtran Corporation P.O. Box 729, Glen Burnie, Md. 21061		11. Contract or Grant No. NASw-2485 13. Type of Report and Period Covered Translation
12. Sponsoring Agency Name and Address National Aeronautics and Space Administration Washington, D. C. 20546		14. Sponsoring Agency Code

15. Supplementary Notes

Translation of: "Acta Technica Academiae Scientiarum Hungaricae", Volume 72, Nos. 1-2, 1972, pp. 3-72.

16. Abstract

Attempts to determine the nature of the movements which can be made in various operational states from the midpoint of the rotating shaft in the bearing plane within limits determined by the bearing race on the one hand and by the load-induced deformations on the other. Evidence is obtained that in the case of a rotating mass balanced with respect to its own axis the point of application of the effective force is located at a single midpoint. The calculations of Stribeck for a bearing with clearance in the case when a loaded ball is in an unstable state are extended to the case of loaded balls in a stable state. It is thus shown that the so-called point load does not exist in even the simplest load arrangement. On the contrary the outer race, up to a certain speed, is acted upon at a spot determined by the phase angle (which depends on the instantaneous speed) by a hammering force the frequency of which is higher than the r.p.m. of the shaft.

17. Key Words (Selected by Author(s))	18. Distribution Statement
	Unclassified-Unlimited

19. Security Classif. (of this report)	20. Security Classif. (of this page)	21. No. of Pages	22. Price
Unclassified	Unclassified	69 67	5.50

ELASTIC VIBRATIONS IN ROLLER BEARINGS[1] I. THE ROTATING MASS IS BALANCED WITH RESPECT TO ITS OWN ROTATIONAL AXIS

B. Szoke[2]

I. INTRODUCTION

/3*

In investigating roller bearing vibrations it is important to pay special attention to the causes of such phenomena. Juergensmeyer [2] is concerned with vibrations caused by faults in finishing and mounting. According to the assumptions of Perret [3, 7] and Meldau [9] the deformations occurring under load can also be considered as contributing to vibrations. Szoke [10, 25-28] points out that "kinetic" vibrations can also occur in a roller bearing presumably free of flaws and deformation. Now, since the notion of deformation has acquired a special meaning in theoretical explanations since Stribeck [1] published his findings, and since we must actually deal with deformation at all times as a consequence of load, investigation of the causes of the vibrations conditioned by deformation is indicated and very promising. The question deserves to be treated even more because the above mentioned authors, who have dealt with the question, have analyzed this subject in connection with these bearings for only the rarest case of very small rotational rates (zero rotation rate), and because in the final analysis their conclusions differ from one another [8].

/4

So it is necessary to treat the problem in greater detail in order to determine what is essential, including all possible operating states.

Our explanations have the purpose of describing the microgeometric phenomena so deeply and thoroughly that within the framework of a general solution all parameters characteristic of bearing construction on the one hand and of operating states on the other can be considered.

II. FUNDAMENTAL CONDITIONS

In the usual analysis of the proper dimensions of rolling bodies it is customary to represent a roller bearing without play and also to accept the

---

[1]This work, submitted under the heading "Microscope", won the prize awarded by the Hungarian Academy of Sciences

[2]B. Szoke titl. Universitaetsdozent, XVIII, Batthyany u. 139, Budapest, Hungary

*Numbers in the right hand margin indicate pagination in the foreign text.

simplification that the midpoint of *one* ball is struck exactly by the line of application of the external force. Now, however, in practice there is no bearing without play and thus the shaft, in relation to the outer race, is only in a stable state if at least *two* balls and generally several *pairs of balls*, with a greater load, are in contact with the race (Figure 1). At first (up to Section XI) the assumption, in the sense of theoretical research common at the turn of the century, that the Hertzian deformations occur only on the ball surfaces, but with the racer surfaces maintaining their exactly circular form, will be followed.

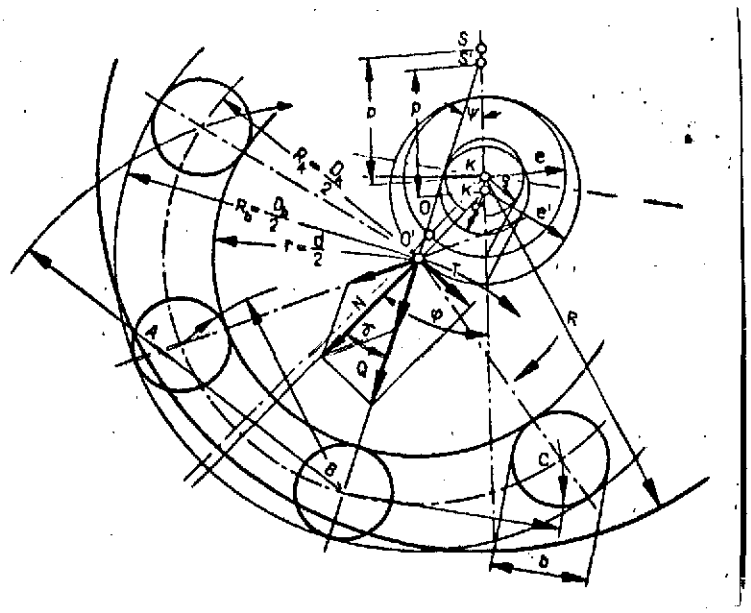

Figure 1. The Deformation Assumed to be Basic (Position at First Moment of Tilting)

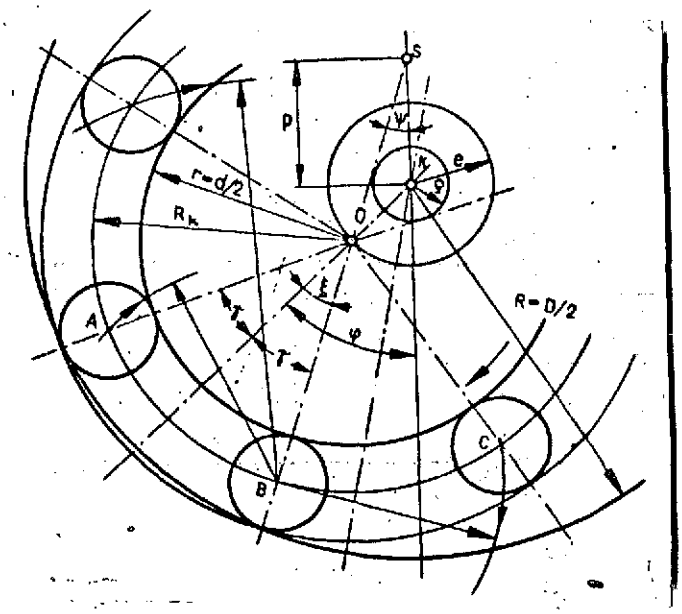

Figure 1a. Beginning of Tilting in the Case Without Deformation

In addition we shall also accept the assumption that the rolling bodies in the unloaded state touch the inner race and that the clearance is found between the outer circumference of the balls and the outer race. Furthermore the rolling bodies will be briefly designated below as rollers or as balls, without consideration of the fact that the deformation of the balls is relatively greater, and that therefore it is more important to consider the tolerance of roller bearings.

Under these assumptions the midpoint 0 of the rotating shaft along with the cage can describe a circular movement around midpoint K of the outer race of such a type that the eccentricity of the race in the unloaded position turns out to be smaller, while it is greater under load by the mass of the flattening deformation of the balls (Figure 1a).

For better understanding Figure 2 represents the geometric position for the case where the midpoint of the outer circumference of the balls is shifted radially from the midpoint K of the outer race to point 0 in such a way that only two balls remain in contact with the outer race.

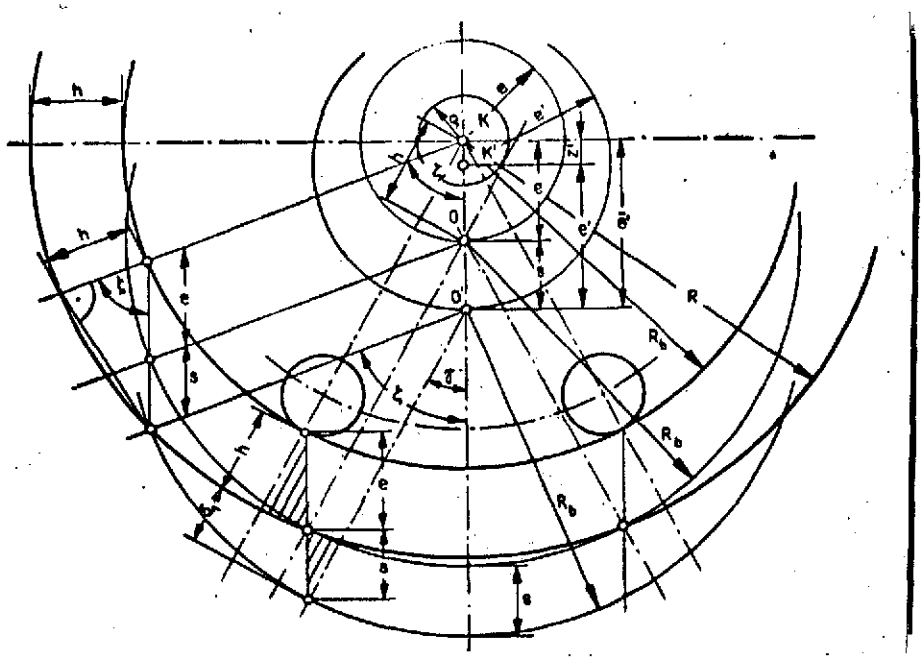

Figure 2. Geometrical Relationships as a Consequence of Deformation

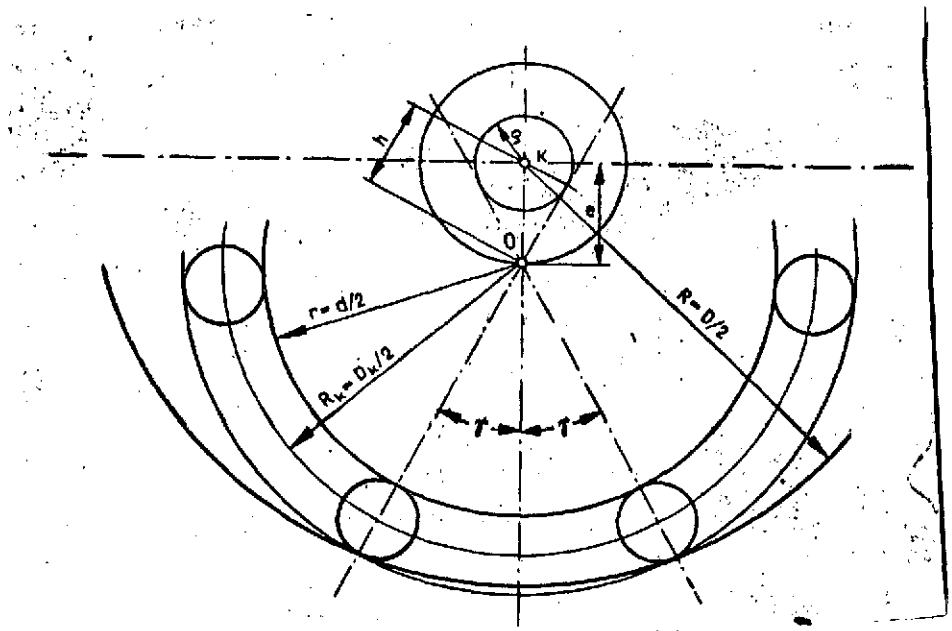

Figure 2a. Geometric Relationships Without Deformation

According to this figure the eccentricity amounts to /7

$$KO = e = \frac{h}{\cos\gamma}, \tag{1}$$

where

$$h = e\cos\gamma$$

means the radial tolerance in the unloaded state which vanishes in the balls in contact.

As a result of a deformation δ_1 of the balls of the first bearing pair of balls, there is a settling in a loaded state by the mass s of the shaft midpoint from position 0 into the new position 0'. The following equation is now valid for this

$$KO' = \bar{e}' = e + s = \frac{h+\delta_1}{\cos\gamma}, \tag{2}$$

where consideration of equation (1) leads to

$$\delta_1 = s\cos\gamma \tag{3}$$

With settling s and deformation δ pertaining to any arbitrary angle $\xi = 2(n + 1)\gamma$ we get:

$$e + s = \frac{h+\delta}{\cos\xi}. \tag{2a}$$

From the figure we can determine that angular opening 2ζ on the circumference of the balls, the legs of which embrace the balls in contact with the race in the case of a shaft settling caused by deformation.

In the sense of equation (2a) that angle ζ should be found at which the deformation of the ball is equal to zero, i.e., where

$$e+s \doteq \frac{h}{\cos\zeta}$$

and from which consideration of equation (1) produces the equation

$$\cos\zeta = \frac{h}{e+s} = \frac{e\cos\gamma}{e+s} = \frac{\cos\gamma}{1+s/e} \tag{4}$$

In this equation all variables are understood as approximate values; this approximation is characterized by the assumption that the corrected eccentricity $e' = e + s - z'$ is really very small in proportion to the radius of the outer race, an assumption which proves to be correct during the course of our explanations.

III. DESIGNATIONS OF THE MOST IMPORTANT CONCEPTS (In Reference to Figures 1 and 2) /8

$d = 2r$ = diameter of the inner race which is assumed to be firm (deformation free); at the same time d is the diameter of the inner circumference of the ball race;

b = diameter of balls describing a planet wheel movement;

$D_k = 2R_k = d + b$ = mean diameter of the ball cage;

$D_b = 2R_b = D_k + b = d + 2b$ = outer circumferential diameter of the unloaded balls;

h = radial bearing play in unloaded state which cannot be directly measured in the case of an odd number of balls;

$D = 2R = d + 2b + 2h = D_k + b + 2h = D_b + 2h$ = diameter of the firm (deformation free) outer race which is at the same time in contact with the balls inside the load arc;

z = number of balls;

$\gamma = 180°/z$ = one-half the distribution angle of the balls;

$e = h/\cos\gamma$ constantly measurable distance [= eccentricity] between the midpoint K of the outer race and the midpoint 0 of the inserted *unloaded* ball cage;

s = settling of shaft midpoint 0 measured at the partition lines of the load arc angle, caused by the deformation of the loaded balls;

$\bar{e}'$ = eccentricity around point K in loaded state;

e' = eccentricity around point K, enlarged by deformation, where the distance $KK' = z'$ = same as osculating circle with radius e';

$\delta_1\delta_2\delta_3 \ldots$ = Hertzian computed value of the oblateness brought about by deformation of the first, second, third, etc., pairs of balls, which at the moment are in a symmetrical position to the bisection lines of the load arc;

ζ = half angle of the load arc;

ξ = half sector angle of the bearing balls within the load arc; always a whole number multiple value of angle γ;

ρ = h tan γ = e sin γ = radius of the basic circle touched tangentially by the vectors of the two neighboring, *unloaded* balls touching the race, where these same vectors enclose the indicated basic circle during rolling;

ρ' = e sin ξ radius of the basic circle assigned to the two load carrying balls in the outermost position within the load arc;

n = rotations per minute of the shaft rotating around midpoint O;

$\omega = n\pi/30$ = rotating angle velocity of the same shaft;

$n_k = nd/(D + d) \approx nd/(2D_k)$ = number of revolutions per minute of the ball cage, simultaneously the speed of rotation of the shaft midpoint 0 on the circular path disposing of an eccentricity of e';

$\omega_k = \omega d/(D + d) \approx \omega d/(2D_k)$ = angular velocity of the rotating ball cage and midpoint 0;

G = weight of the mass m rotating around the shaft center O with rotational number n and balanced on the shaft midline;

g = gravitational constant;

F = components of the force operating from outside on the bearing (e.g., belt tension, tooth pressure), assumed to be unaltered;

$\overline{P} = \overline{G} + F$ = resultant of the specific weight and the external force components operating on the bearing;

m = mass reduced on the shaft midpoint and balanced on the shaft midline;

$\overline{\alpha} = P/m$ = mass acceleration;

$C = me\omega_k^2$ = centrifugal force as an opposing power of the centripetal force caused by the revolving motion on the unloaded bearing;

$C' = me'\omega_k^2$ = centrifugal force on a loaded, eccentric bearing;

$\overline{c} = e\omega_k^2$ = centrifugal acceleration on an unloaded bearing;

$\overline{c}' = e'\omega_k^2$ = centrifugal acceleration in a loaded, eccentric bearing;

$\overline{Q} = \overline{P} + \overline{O}$ = resulting force, without regard to ball deformation;

$\overline{Q}' = \overline{P} + \overline{O}'$ = resulting force with consideration of ball deformation; /9

$\overline{i} = Q/m$ = resulting acceleration without consideration of ball deformation;

$\overline{i}' = Q'/m$ = resulting acceleration with consideration of ball deformation;

$p = KS = \overline{\alpha}/\omega_k^2$ = distance from pole S (of the midpoint of the forces) from the midpoint K of the outer race;

ψ = phase angle of the rotating or rocking motion;

ϕ = phase angle of the shaft midpoint O when rotating around midpoint K;

$\overline{n}$ = normal components of the acceleration $\overline{i}$ of the imaginary mass m concentrated in shaft midpoint O, passing through the midpoint K;

$\overline{t}$ = tangential component of acceleration $\overline{i}$;

$N = m\overline{n}$ = normal force in the straight symmetrical lines of the load arc, which causes the ball deformation;

$T = m\overline{i}$ = the tangential force operating on the imaginary and circulating mass concentrated at point O, causing the rotating motion and the rocking motion;

$D_T = 2R_T$ = diameter of the Thales circle through which the length of the agitation is determined (Figure 23).

y = length of the oblique plane in the Thales circle (i.e., tangential or impact amplitude);

x = radial or crown amplitude of the tilting oscillation (Figure 21);

α_0 = angle of inclination of the oblique lines occurring at the place of the rotating path with the force line in the case of zero revolutions with a firm ball support;

α = the same angle of inclination with a movable ball support;

$u = y \cos \alpha$ = "height of fall" in the Thales circle;

$+ k$ = proportionality factor through which the ratio of the diameter of the inner race to the ball diameter is determined; important for computing the Hertzian oblate radius;

$- K$ = proportionality factor through which the ratio of the diameter of the outer race to the ball diameter is determined;

μ = friction of coefficient between ball surface and race surface;

μ_1 = coefficient of friction between ball surface and cage surface;

$\overline{\rho}$ = angle of friction of the roller bearing;

M = rolling friction moment of the balls;

f = rolling friction spoke of the balls;

θ = diameter of the oblate circle of the ball.

IV. THE ROLLER BEARING AS PLANETARY GEARING

In the bearing with clearance, the shaft midpoint 0 can shift in any direction relative to the midpoint K of the outer race. In a stable position in the loaded state it can be imagined with the assistance of the symmetrical arrangement that a hinged spoke between the midpoint K of the outer race (with diameter D) and the midpoint O' of the inner race (with diameter d) is just as long as the eccentricity $\overline{e}'$. This relationship is clearly visible from the somewhat distorted, geometric Figure 3 in which the bearing midpoint O' of two balls (ball diameter b) represents the cage or its center of gravity.

Since the masses on the same axis, rotating around axis O' with angular velocity ω, are balanced, in the computation of the centrifugal force operating on radius $\bar{e}'$, the circulating rotational angle of velocity ω_k of the center of gravity O' of the mass m must be considered. The number of revolutions of spoke $\bar{e}'$ and of the cage can be determined by reflecting that first the entire system, in which presumably all parts are locked in relationship to one another, is allowed to rotate fully and then, after the restriction is removed, the outer race with diameter D is allowed to return to its original position. /10

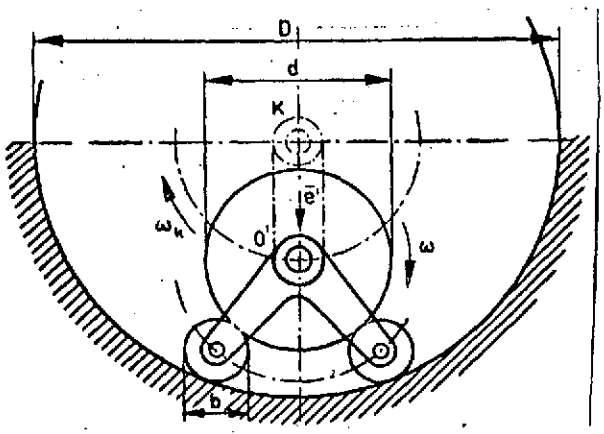

Figure 3. A Planetary System as an Explanation for a Roller Bearing With Radial Clearance

	Rotational speed Imag. spoke $\bar{e}'$	Inner race Ø d	Ball Ø b	Outer race Ø D
Full revolution of locked system	+ 1	+ 1	+ 1	+ 1
Outer race with Ø D returned to original position with immovable spoke $\bar{e}$	0	$+\frac{D}{d}$	$-\frac{D}{b}$	- 1
The resulting number of revolutions.	+ 1	$1+\frac{D}{d}$	$1-\frac{D}{b}$	0

Thus the arm $\bar{e}'$ (and also the cage) in *one* revolution of the inner race (diameter d) makes

$$\frac{1}{1+D/d}=\frac{d}{D+d}$$

revolutions, i.e., when the inner race makes n revolutions, the number of revolutions of spoke $\bar{e}'$ (and of the cage) amounts to

$$n_k = n\frac{d}{d+D}. \tag{5}$$

Even if the distance of point O' from point K is extreme, this formula retains its validity. In regard to ball bearings it is permissible to insert the doubled mean diameter of the cage in place of (d + D); this approximate value /11 is the result of ignoring spoke $\bar{e}'$

$$n_k = n\frac{d}{2D_k} \tag{6}$$

and the angular velocity of the revolving cage amounts to

$$\omega_k = \frac{n_k\pi}{30} = \frac{n\pi}{30}\frac{d}{d+D} = \omega\frac{d}{d+D} \approx \omega\frac{d}{2D_k} \tag{7}$$

Analogously the rotational speed of the balls, if the inner race makes n revolutions, amounts to:

$$n_b = n\frac{1-(D/b)}{1+(D/d)} = n\frac{d}{D+d}\frac{D-b}{b} = -n_k\frac{D-b}{b} \approx -n\frac{d}{2D_k}\frac{D-b}{b}. \tag{6a}$$

V. AN AUXILIARY THEOREM

The auxiliary theorem derived here amounts to a rigid system of mass points which rotates around an arbitrary axis in any homogeneous force field.

We assume that a plane, found at a right angle to any axis k, rotates around this axis with an angular velocity ω_k (Figure 4a). Point O of the mass m is located at a distance e from the rotational midpoint K of the plane /12 mentioned. Point O is the point of application of the specific weight G and of the outer force F, since the direction of this force F remains unchanged, as a result of which the direction of the resultant P remains unchanged.

But since the centrifugal force C operating at point O changes its direction, the result is a final resultant force $\bar{P} + \bar{C} = \bar{Q}$, the magnitude and direction of which is changeable during the rotation of the plane.

In Figure 4b we have presented the vector diagram for the forces operating on the mass unit, i.e., for accelerations

$$\frac{P}{m} = \bar{a},$$

(as resultants of accelerations G/m = g, and F/m = f),

$$\frac{C}{m} = e\omega_k^2 = \bar{c}\,,$$

$$\frac{Q}{m} = \bar{i}$$

Since the magnitude and direction of the vector $\bar{a}$ in the vector diagram are constant and since vector $\bar{c}$ describes a circular line with radius $\bar{c}$ around midpoint K_V, viz., in a plane perpendicular to axis k, the resulting acceleration $\bar{i}$ is always a generatrix of an oblique circular cone whose height is just $\bar{a}$ and whose height of center forms the angle λ_0 with the rotating plane. In the vector triangle which contains the angle λ_0, we find the minimum value $\bar{i}_{min}$ and in another vector triangle with angle $(180° - \lambda_0)$ the maximum value of the acceleration i_{max}.

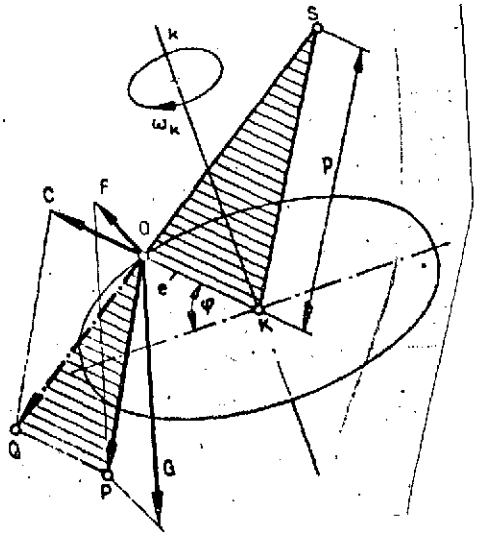

Figure 4a. Midpoint of the Forces (Force Pole) of the Mass Points of a Plane Which Rotates Around Any Axis at Right Angles to This Plane.

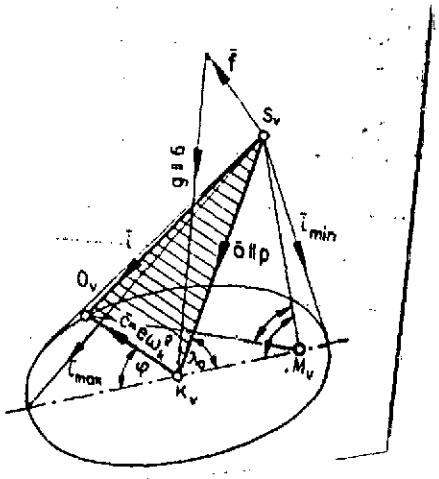

Figure 4b. Vector Diagram.

Since the vector triangle OPQ (forces) and $S_V K_V O_V$ (accelerations) are similar in every position of point O of triangle SKO, we get

$$p : e = \bar{a} : e\omega_k^2$$

for the polar distance, and with the assistance of equations (5) and (7), we can write:

$$p = \frac{\bar{a}}{\omega_k^2} = \left(\frac{30}{n_k \pi}\right)^2 \bar{a} = \frac{\bar{a}}{n_k^2}\left(\frac{30}{\pi}\right)^2 \cdot \left(\frac{d+D}{d}\right)^2 = \frac{91\bar{a}}{n_k^2}\left(\frac{d+D}{d}\right)^2 \approx \frac{91\bar{a}}{n_k^2}\left(\frac{2D_k}{d}\right)^2. \qquad (8)$$

This is thus the equation through which pole S (midpoint of forces), oriented to the rotating plane and remaining rigid, is determined. The similarity of the mentioned triangle produces the principle that, as long as magnitudes $\bar{a}$ and ω_k remain unchanged, every resulting force of any mass point of the rotating plane passes this pole S. /13

We choose the corresponding position of acceleration $\bar{i}_{max}$ as the initial position in which to determine the magnitude of an acceleration $\bar{i}$ belonging to any phase angle ϕ.

In triangle $S_V M_V O_V$ side $S_V M_V$ is also a perpendicular drawn to the revolving surface, i.e., $\sphericalangle S_V M_V O_V = 90°$, and therefore:

$$\overline{S_v O_v}^2 = \bar{i}^2 = \overline{S_v M_v}^2 + \overline{O_v M_v}^2.$$

From the right triangle $S_V M_V K_V$ we get

$$S_v M_v = \bar{a} \sin \lambda_0 ,$$

and from the general triangle $O_V M_V K_V$ it follows that

$$\overline{O_v M_v}^2 = \bar{c}^2 + \overline{K_v M_v}^2 + 2\bar{c}\,\overline{K_v M_v}^2 \cos \varphi ,$$

i.e.,

$$\bar{i}^2 = \bar{a}^2 \sin^2 \lambda_0 + \bar{c}^2 + \overline{K_v M_v}^2 + 2\bar{c}\,\overline{K_v M_v} \cos \varphi .$$

Now since

$$K_v M_v = \bar{a} \cos \lambda_0 ,$$

then

$$\bar{i}^2 = \bar{a}^2 \sin^2 \lambda_0 + \bar{c}^2 + \bar{a}^2 \cos^2 \lambda_0 + 2\bar{a}\bar{c} \cos \lambda_0 \cos \varphi ,$$

i.e.,

$$\bar{i}^2 = \bar{a}^2 + \bar{c}^2 + 2\bar{a}\bar{c} \cos \lambda_0 \cos \varphi . \qquad (9)$$

As initial position of the phase angle ϕ was chosen the symmetrical plane containing the angle λ_0, and consequently equation (9) retains its validity in both rotating directions.

In connection with spindle bearings with a vertical axis, which are only loaded by their specific weight, we get angle

$$\lambda_0 = 90°$$

and thus:

$$\bar{i}^2 = \bar{a}^2 = \bar{c}^2 . \qquad (10)$$

In connection with radial ball bearings with a horizontal axis (journal bearings), if the bearing reaction occurs in a direction normal to the axis, we get

$$\lambda_0 = 0$$

and thus

$$\bar{t}^2 = \bar{a}^2 + \bar{c}^2 + 2\bar{a}\bar{c}\cos\varphi \,. \tag{11}$$

Since in practice the latter case is usually found, we shall restrict ourselves in the following to this case alone.

It seems useful to summarize the relationships expressed in equations (8) and (11) as follows: /14

(1) A single pole (midpoint of forces) S in space belongs to all points of the plane rotating about the axis; the distance of this pole from the rotating midpoint of the plane is $p = \bar{a}/\omega_k^2$ and the direction of this distance is parallel to the acceleration vector $\bar{a}$.

(2) The poles of two planes parallel to one another lie on one straight line parallel to the rotational axis.

(3) When the increasing acceleration $\bar{a}$ approaches infinity or the diminishing angular velocity approaches the zero value, a midpoint S of the forces, in accord with equation (8), tends toward infinity, viz., in the direction of acceleration $\bar{a}$.

(4) In case the position of the mass point O in the rotational plane changes with a rigid rotational axis k, the position of pole S remains unaffected by the change in eccentricity e. But if the rotational axis k is shifted parallel to itself, the polar distance is also shifted parallel to itself.

(5) If the angular velocity changes during one revolution, and if acceleration $\bar{a}$ still remains unaltered, the line of the polar distance p remains in its position, and only its magnitude suffers a change inversely proportional to the square of the velocity.

(6) When force actions occur in the main plane normal to the axis of a radial ball bearing, the pole also remains in this main plane, and at the same time the equation (8) determining the position of the pole S contains the most important data about the bearing in addition to the most important characteristics of the operational states.

(7) When the rotating mass is not balanced on its own axis (see Part II of this report), it is not the angular velocity ω_k of the rotation, but the

angular velocity ω of the rotating movement which is decisive in the computation of the pole distance p:

$$p = \frac{a}{\omega^2} . \tag{12}$$

VI. THE NORMAL AND TANGENTIAL FORCES OPERATING AT THE AXIAL CENTER OF GRAVITY OF THE SYSTEM IMAGINED TO BE ROTATING IN THE BEARING MID-PLANE

Although the auxiliary theorem introduced in connection with Figure 4 offers a certain insight in the most general cases, we would like to treat here only the case most often occurring in practice in which the axis k is horizontal and is affected by a perpendicular, spatial, external force.

For the sake of simplicity we have chosen for the analysis of the forces operating on the bearing the symmetrical arrangement presented in Figure 4c, since in this case the two bearings are subject to the same load, and therefore we can satisfy ourselves with an investigation of only one of them. /15

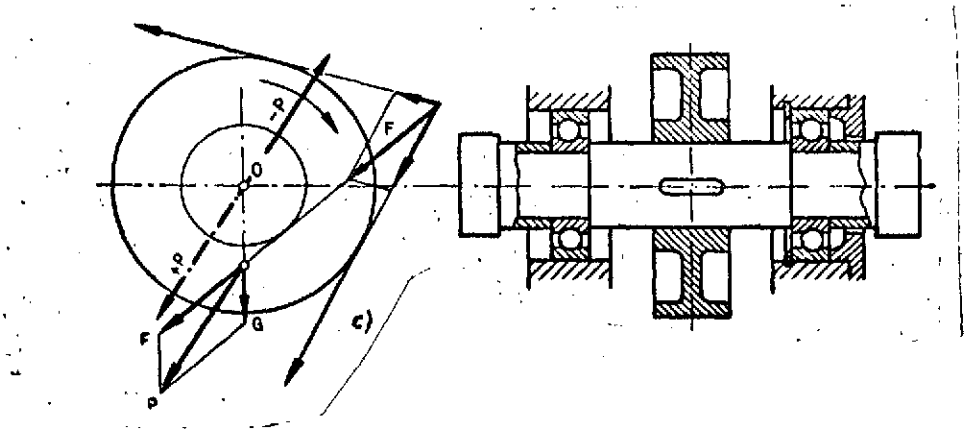

Figure 4c. The Force Operating In The Bearing Plane

In the case of a bearing without clearance we must, prescinding from the vibrations occurring as a result of the finite number of rolling bodies (see sources [27] and [28]), calculate with a uniform rotation of the shaft with the angular velocity ω. During operation the resultant of the tensile forces occurring in the loose and tight belt streams on the pulley in a line normal to the axis in space, but twisted, with the normal transversal forming the spoke of the tilting moment developed. All individual specific weights (shaft and concomitant pulley, shaft couplings at both ends of the shaft, inner races in both roller bearings, both cages and both rolling body rims) operate in a vertical straight line cutting the axis, the straight line being found in the midplane of the system. The line of application of the resultant P, stemming from the specific weight G and the operative tractive force F, is also twisted in relation to the axis. If we now imagine at point O the two forces operating with one another in balance to be in a position parallel to the mentioned twisted line, we are already clear about the position of the external forces

loading the inner races and about the moments to be transmitted by the two shaft couplings. Actually in the figure only the forces working at one bearing position are presented. Pole S as a midpoint of the forces is found for a bearing without clearance on the line of attack of the force P affecting the concentrated mass m thought of as being in the midplane of the bearing. Since this time the center of gravity of the mass m is located in the rotation midpoint, the centripetal forces operating on the mass points of the system are in equilibrium during rotation.

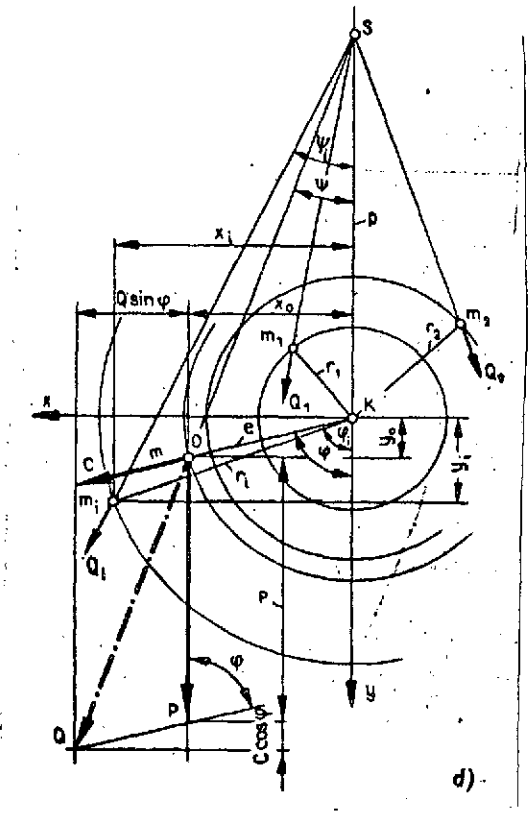

Figure 4d. The Mass Point Substituting for the Rotating System

In the presence of bearing clearance, but lacking a load causing a tangible deformation on the roller bodies, the shaft midpoint O, simultaneously the center of gravity of the system thought to be in the bearing midplane and rotating with angular velocity ω, is constrained to follow a circular motion of angular velocity ω_k along a circular line of radius KO around midpoint K of the outer race, in accord with Figure 1a.

Our auxiliary theorem is only temporarily valid for the individual mass points of the system in the sense of the derivation. Here we wish to show that the same theorem is also valid for the mass midpoint of the rotating system. The proof is directed only to our particular case, namely, when the plane of the rotating system is in a right angle to the line accommodating itself to the rotational midpoint K.

With the drawings in Figure 4d we can state that the system consisting of the mass points m_1, m_2... m_i rotates around midpoint K. /16

We wish to prove that the vectorial sum of the forces operating on the individual mass points

$$\Sigma \bar{Q}_i = \bar{Q}$$

lies on one line accommodating itself to the mass midpoint O and the force midpoint S; the magnitude of the resultants is determined by mass $\Sigma m_1 = m$ and the acceleration $\bar{i} = \bar{a} + \bar{c}$.

We now wish to express the sum of the projections resulting from the operating forces in the directions x and y and also the resultant of both projections as follows: /17

$$\Sigma Q_l \sin \psi_l = \Sigma P_l + C_l \cos \varphi_l = a \Sigma m_l + \omega_k^2 \Sigma m_l r_l \cos \varphi_l .$$

In agreement with the drawings in the figure and with consideration of the definitions it follows that

$$\Sigma m_l = m$$

and after introducing

$$\Sigma m_l r_l \cos \varphi_l = \Sigma m_l y_l = m y_0$$

we get

$$\Sigma Q_l \sin \psi_l = ma + \omega_k^2 m y_0 .$$

In an analogous way we obtain the sum of the force projections in the direction x

$$\Sigma Q_l \sin \varphi_l = \omega_k^2 \Sigma m_l r_l \sin \varphi_l = \omega_k^2 m x_0 .$$

In this way the resulting force Q can be expressed as follows

$$Q = \sqrt{m^2(a + \omega_k^2 y_0)^2 + m^2(\omega_k^2 x_0)^2} ,$$

i.e.,

$$Q = m \sqrt{a^2 + 2a y_0 \omega_k^2 + \omega_k^4 y_0^2 + x_0^2 \omega_k^4} .$$

With consideration of the position of the mass m concentrated in the mass center O

$$e^2 = x_0^2 + y_0^2$$

is valid for the eccentricity, and therefore

$$Q = m \sqrt{a^2 + 2a y_0 \omega_k^2 + e^2 \omega_k^4} .$$

In the sense of the figure $y_0 = e \cdot \cos \phi$ and thus

$$Q = m \sqrt{a^2 + 2ae\omega_k^2 \cos \varphi + (e\omega_k^2)^2} .$$

In this way we have proven our statement about the mass midpoint, namely with consideration of the similarity of triangles

$$\triangle OPQ \sim \triangle SKO ,$$

the expression (e ω^2) is equal to the resulting acceleration, and thus preserves its validity for the center of gravity of the rotating system on the basis of the similarity of the proportion (8)

$$p : e = a : e\omega_k^2$$

The external load is transmitted from the outer surface of the inner race to the rollers, but the rollers also take on the reaction load from the inner surface of the outer race, causing deformation of the rollers, and thus the shaft midpoint is displaced into the new position O', which at the same time means a change in the theoretical rotational orbit (Figure 1). In the sense of the already derived theorem, however, we can determine the resulting force operating on the shaft center, i.e., on the mass midpoint, at any arbitrary position of point O'. /18

In computing the forces operating on the bearing, we would like to prescind for a moment from the real rotational movement of the rollers and assume that the shaft, the rollers and the cage affect a circling motion of rotation n_k as one unit in accord with equation (6) (as can also be demonstrated by means of certain stroboscopic photographs, in certain cases this brings about a sliding motion of the rollers).

According to the reflections in the second part of this paper, it would be possible to bring the rotational motion of one roller about its own axis into the computations. Nevertheless, in comparison to the total rotating system its mass is, so to say negligible, and in addition it is quite uncertain how far the rollers really can perform the revolutions n_b expressed in equation (6a) because of the braking operation of the lubricant, and therefore to include the specific revolution of the rollers in this consideration would be a superfluous difficulty in computation.

When friction is temporarily left out of consideration, the line of application of the reactive force exerted on the individual rollers through the inner surface of the outer race as a compulsory path goes through the midpoint of the rollers. Thus on the one side the resultant of all these reactive forces and on the other side the normal force components N of the force Q passing through the rotational midpoint K are found to be in equilibrium with each other. However, during the circular motion the tangential component T also exerts its influence, and we shall discuss this below.

It can be seen from Figure 3 that the effect of the forces causes the shaft midpoint O to make a circulating movement of radius KO' about the rotational midpoint K of the outer race. We shall now examine the way in which this compulsory revolution is affected by one deformation of the ball, and whether and how the above described circulating movement proceeds or changes. For this it is necessary to know the normal and the tangential components of the force operating on the midpoint at one position on the circulating rotational path: after all, the deformation is caused by the normal force component and the (momentaneous) motion is produced by the tangential force component.

Figure 5a shows the accelerations $\bar{i}$ operating on the center of gravity 0 and its components, normal $\bar{n}$ and tangential $\bar{t}$, in its passage from position $\phi = 0$ to position $\phi = \pi$ vectorially, and Figure 5b shows the same configuration /20 in the course of the other hemispherical area from π to 2π. The figure leads to the determination that the components mentioned can be found correctly with the help of a Thales circle if the acceleration vector $\bar{a}$ is chosen as the diameter of this circle.

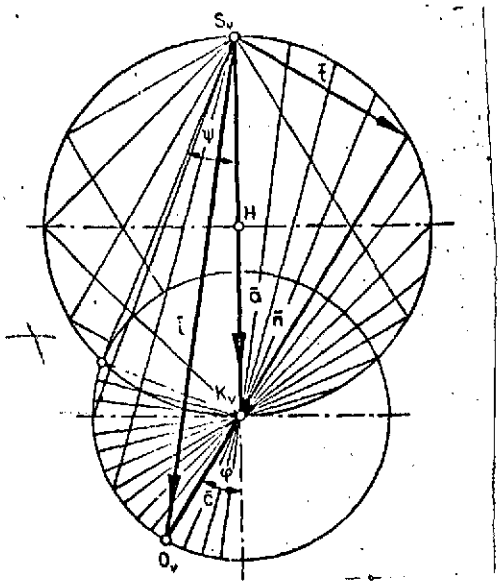

Figure 5a. Vector Diagram of Acceleration $\bar{i}$ and its Rectangular Components During the First Half Revolution. Terminal Polar Distance.

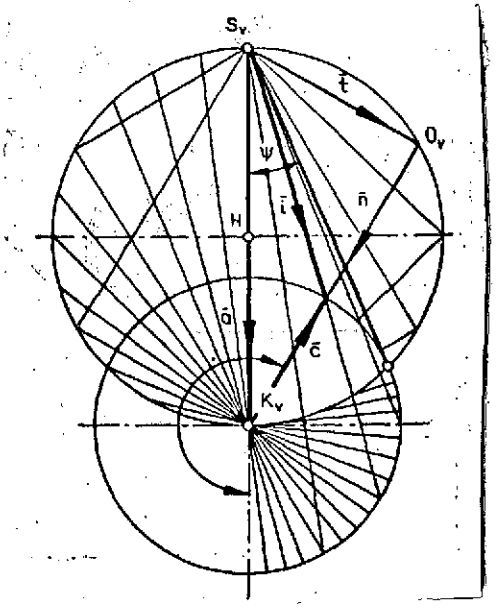

Figure 5b. Position of the Same Vectors During the Second Half Revolution.

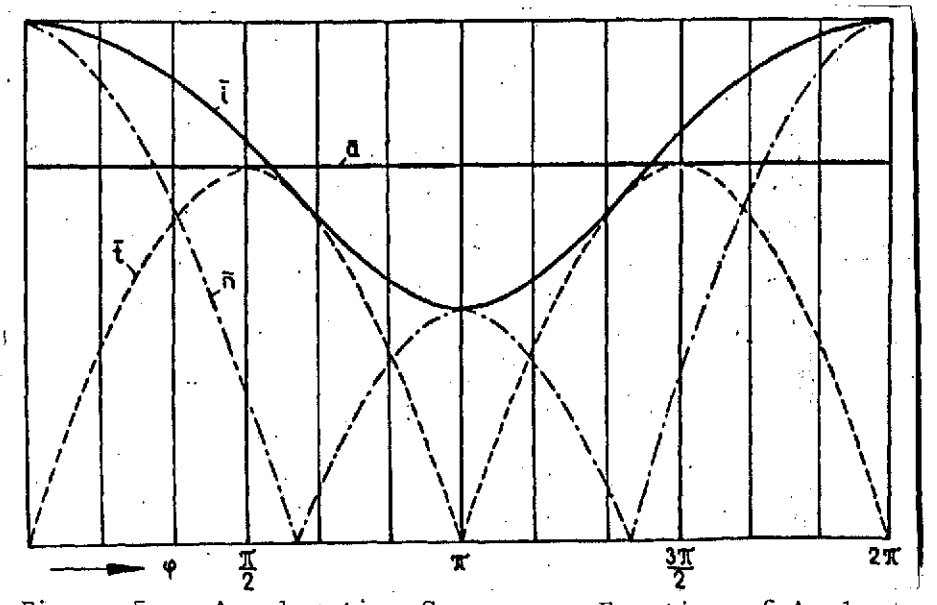

Figure 5c. Acceleration Curve as a Function of Angle ϕ (With the Circular Area Straightened Out).

Depending on the magnitude of the relationship of vectors $\bar{a}$ and $\bar{c}$, the following cases can be produced:

Case 1. $\bar{a}/\bar{c} > 1$; $p > e$; pole S lies at the terminal

The components mentioned are produced from Figure 5a as follows:

$$\bar{n} = \bar{a}\cos\varphi + \bar{c}, \tag{13}$$

$$\bar{t} = \bar{a}\sin\varphi. \tag{14}$$

Table of Individual cases:

φ	$\cos\varphi$	$\bar{i}$	$\bar{n}$	$\bar{t}$
0^0	1	$\bar{a}+\bar{c}$	$\bar{a}+\bar{c}$	0
$\frac{\pi}{2}$	0	$\sqrt{\bar{a}^2+\bar{c}^2}$	$\bar{c}$	$\bar{a}$
$\bar{c} \perp \bar{i}$	$-\frac{\bar{c}}{\bar{a}}$	$\sqrt{\bar{a}^2-\bar{c}^2}$	0	$\bar{i}$
π	-1	$\bar{a}-\bar{c}$	$\bar{a}-\bar{c}$	0

After completion of the second half revolution, values are produced which correspond to the symmetrical axis $S_V K_V$ (Figure 5b). /21

With angle ϕ straightened out we obtain the curves of the accelerations as angular functions according to Figure 5c.

If we compare Figures 5a and 1 with each other, we can establish the following: the (normal) deformation component operating on center of gravity O reaches its highest value when it is superimposed on the radius SK, and if we imagine the case where this component takes the position of a tangent from point S to the circle of radius e, only the tangential force component would be effective.

$$\text{Case 2: } \bar{a}/\bar{c} > 1;\ p = \bar{a}/\omega_k^2 \to \infty.$$

This condition exists when either the acceleration $\bar{a}$ is exceedingly large or when ω_k in comparison to $\bar{a}$ is estremely small. If, e.g., only gravitational is considered as a load, i.e., when $\bar{a} = g$, then the equation for the polar distance is

$$p = \frac{g}{\omega_k^2} = \frac{895}{n_k^2} \tag{7a}$$

and if we accept the value of 1/4 V/min for n_k, we get

$$p = 895 \times 16 = 14{,}32 \text{ km} .$$

If by chance the eccentricity e amounts to only 49 µm at the same time, the ratio

$$p/e = 3 \cdot 10^8 .$$

is produced. In such a case the Thales circle constructed around vector $\bar{a}$ changes into a straight line constructed through point K_v and directed perpendicularly to line $\bar{a}$, and the extremely narrow triangle formed from vectors $\bar{a}$, $\bar{c}$ and $\bar{i}$ turns the centrifugal acceleration $\bar{c}$, in comparison to $\bar{a}$, into a tiny magnitude (the case of the so-called zero revolution), negligible in respect to $\bar{a}$, and thus

$$i = \bar{a} .$$

With the torque angle ϕ we get the normal acceleration component (Figure 6a)

$$| \bar{n} | = | \bar{a} \cos \varphi | \qquad (13a)$$

and the tangential component

$$t = \bar{a} \sin \varphi .$$

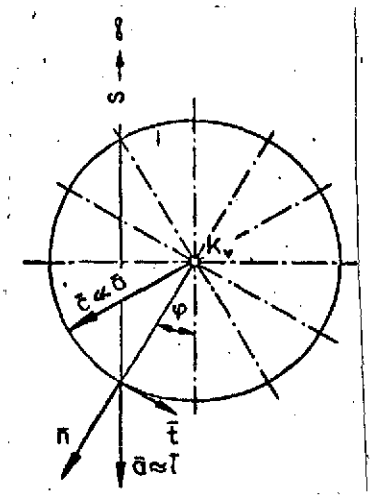

Figure 6a. Accelerations. Nonterminal Polar Distance.

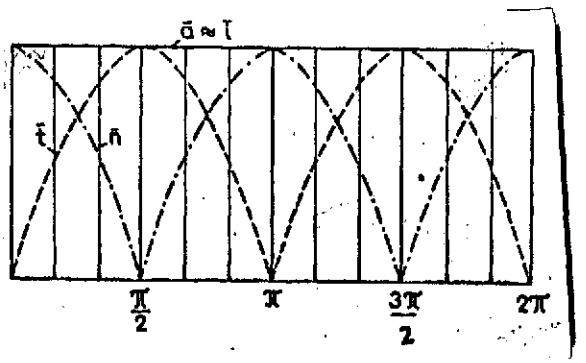

Figure 6b. Acceleration Curve as a Function of Angle ϕ (With Circular Area Straightened Out).

Special cases: /22

φ	$\bar{n}$	$\bar{i}$
0	$\bar{a}$	0
$\frac{\pi}{2}$	0	$\bar{a}$
π	$\bar{a}$	0

The forces are presented in Figure 6b with the leveled angle ϕ.

Case 3: $\bar{a}/\bar{c} = 1$; p = e; Pole S lies on the circular path of the circling movement.

In Figure 7a we can see that the Thales circle, the middle point of which according to the definition lies at the bipartition point H of the acceleration vector $\bar{a}$, touches the other circle with radius e at point S_v from inside.

According to this equation (11) for acceleration $\bar{i}$ takes the following shape:

$$i^2 = 2a^2(1 + \cos\varphi);$$

$$i = 2a\sqrt{\frac{1+\cos\varphi}{2}} = 2a\cos\frac{\varphi}{2}, \tag{15}$$

which moreover corresponds exactly with the geometrical relationships of triangle $S_v O_v O_{v0}$ in Figure 7a.

The normal component of $\bar{i}$ is /23

$$\bar{n} = \bar{a} + \bar{a}\cos\varphi = \bar{a}(1 + \cos\varphi), \tag{16}$$

and its tangential component

$$t = a\sin\varphi.$$

Special cases (see diagram in Figure 7b):

φ	$\cos\varphi$	$\bar{i}$	$\bar{n}$	$\bar{t}$
0	1	$2\bar{a}$	$2\bar{a}$	0
$\frac{\pi}{2}$	0	$\bar{a}\sqrt{2}$	$\bar{a}$	$\bar{a}$
π	-1	0	0	0

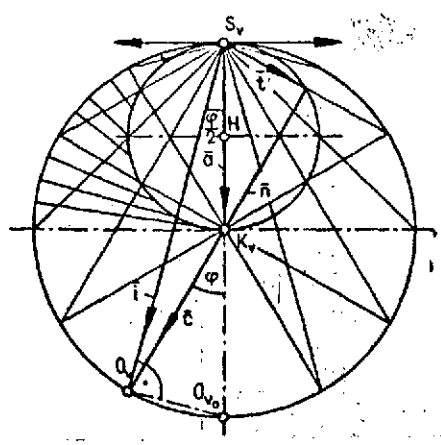

Figure 7a. Accelerations With the Pole on the Rotational Path

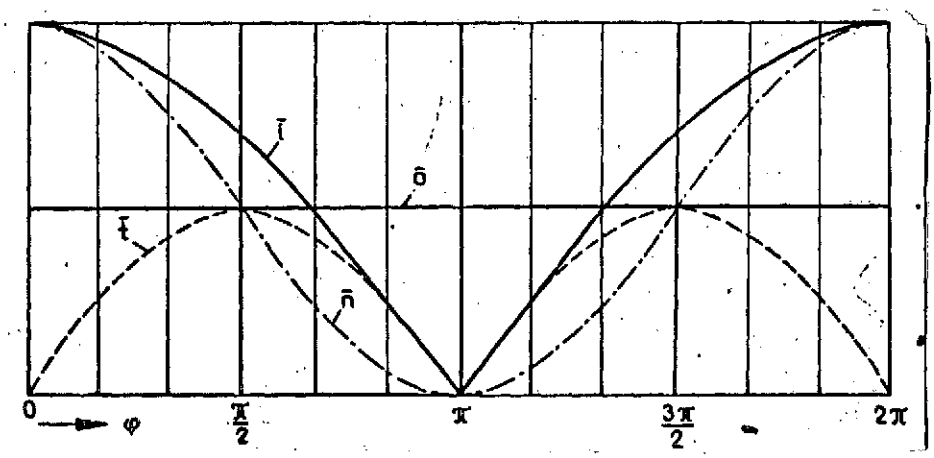

Figure 7b. Acceleration Curve as a Function of Angle ϕ (With Circular Range Straightened)

Case 4. $\bar{a}/\bar{c} < 1$; $p < e$; Pole S lies inside the circle of radius e.

In Figure 5a the position of the acceleration $\bar{i}$ could only be conceived of as being inside angle 2ψ. In Figure 7a this limit was $2\psi = \pi$; according to Figure 8a discussed below acceleration $\bar{i}$ can make a complete revolution up to 2π.

The normal component of $\bar{i}$ is

$$\bar{n} = \bar{c} + \bar{a}\cos\varphi \tag{17}$$

and the tangential component is:

$$\bar{t} = \bar{a}\sin\varphi .$$

Special cases:

φ	$\cos\varphi$	$\bar{t}$	$\bar{n}$	$\bar{\tau}$
0	1	$\bar{a}+\bar{c}$	$\bar{a}+\bar{c}$	0
$\frac{\pi}{2}$	0	$\sqrt{\bar{a}^2+\bar{c}^2}$	$\bar{c}$	$\bar{a}$
π	-1	$\bar{c}-\bar{a}$	$\bar{c}-\bar{a}$	0

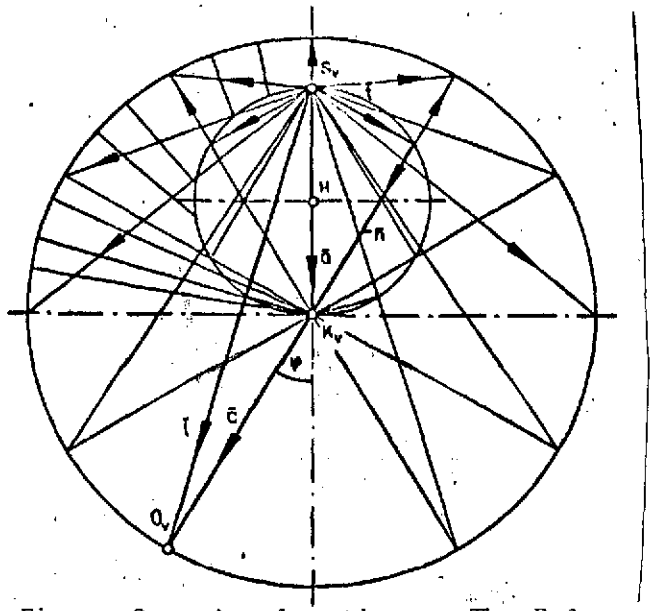

Figure 8a. Accelerations. The Pole in the Center of the Rotational Path

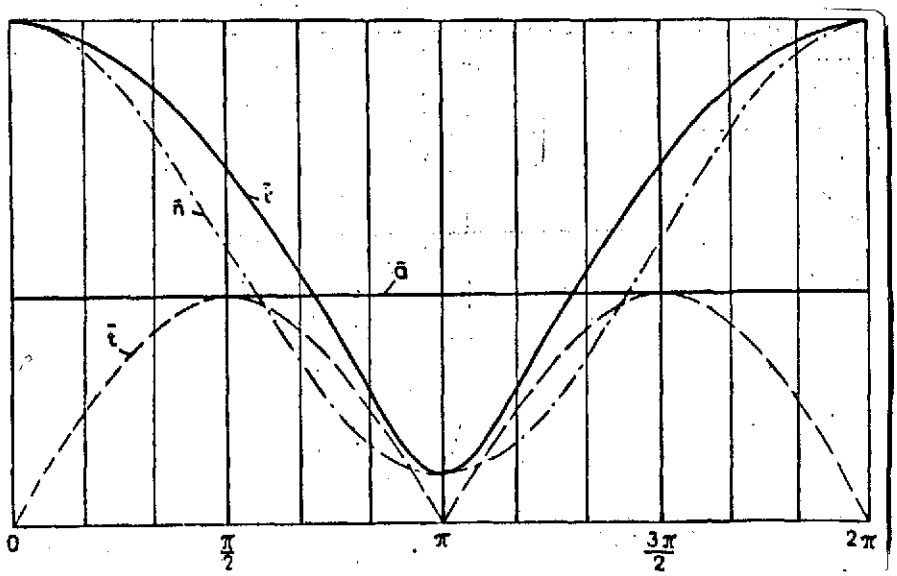

Figure 8b. Accelerations as a Function of Angle ϕ (With Circular Range Straightened Out).

The usual diagram for accelerations as angular functions can be seen in Figure 8b. With an increasing number of revolutions pole S keeps approaching point K, but will only reach this point K in an infinitely large number of revolutions.

For the purpose of symmetry the vector $\bar{a}$ in this section is found in every vector diagram on the central vertical lines. This type of presentation is also to be maintained for the force diagrams. But for the sake of truth it should be mentioned that the position of the pole distance KS = p can take on any arbitrary direction according to the actual operating relationships.

VII. DETERMINATION OF THE LOAD ARC

On the one side the pole distance p and on the other side the magnitude of the load arc caused by the deformation are decisive in producing the movement phenomena of the rotating mass with the center of gravity O in the shaft middle. It should be noted that the pole distance is not dependent upon the rotating mass m; according to equation (8) this distance is a function of the number of revolutions n_k, acceleration $\bar{a}$, raceway diameters D and d (at the outer and inner race), while the load arc 2ζ, according to equation (4), /25 depends upon the following magnitudes:

- on eccentricity e,
- on number of balls $z = 180°/\gamma$,
- on deformation settling s,

and in connection with this latter magnitude the load arc 2ζ is a function of /26 the force $Q_{max} = m\bar{i}$, thus a function of the rotating mass m at the same time.

Eccentricity e is determined only by measurements, while settling s can be determined by measurements or by computation.

1. Determination of Bearing Clearance by Measurements

This determination takes place, for example, by applying the process recommended on the part of the Swedish Ball Bearing Factory [18].

The accuracy of this process is completely satisfactory. In Figure 9 we see the apparatus used for this. At one end the shaft has the weight G. Accordingly the bearing is stressed by a downward directed load consisting of weight G and part of the weight of the shaft itself. The measurement dial m is attached to the bearing housing in such a way that the tip of the instrument is mounted on the shaft as close to the bearing as possible; the hand of the measuring dial is read. With the help of a spring scale r, the shaft is loaded in phases. During this process the position of the measuring instrument is read at every load and recorded. The load is raised until its magnitude reaches the estimated highest value of the original downward directed load.

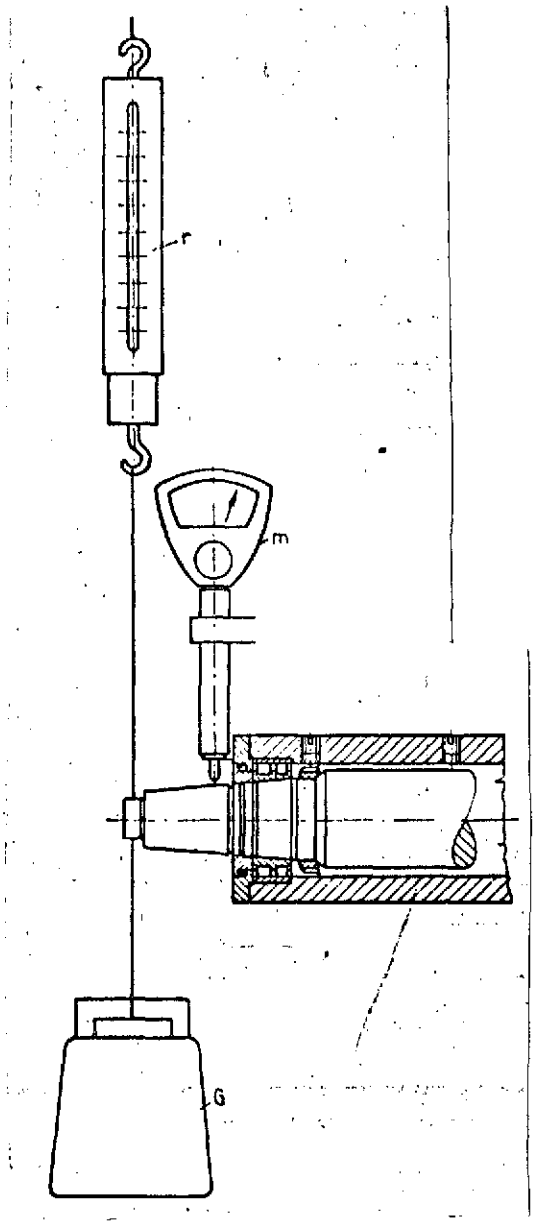

Figure 9. Apparatus for Determining Bearing Play by Measurements.

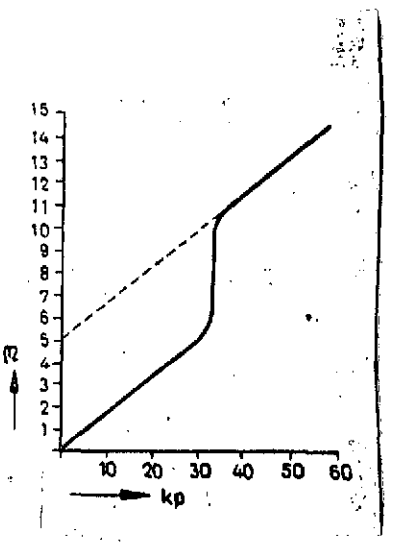

Figure 9a. Load Diagram for the Experimental Determination of the Bearing Play.

The curve to represent the position of the instrument hand (the deformation values) is plotted in the diagram as a function of the spring scale hand positions, from which the bearing clearance can be immediately determined. Thus, for example, it can be determined from Figure 9a that the spring action of the shaft is directed downward from 0 to 30 kgf and upward from about 35 to 60 kgf. These two segments of the mentioned curve are two lines almost exactly parallel to one another; in regard to the small loads involved here, the spring

action can be understood as being only the phenomenon corresponding to the shaft deformation. For the curve segment of values 30...35 kgf, we can assume that the bearing here is unloaded, because these values correspond approximately to the sum of the load weight and the specific weight, so that the jump in the line is equal to the bearing clearance. Without such a bearing clearance, the curve would take the shape of an uninterrupted straight line (between 0 and 60 kgf). Logically the bearing clearance can be read from the ordinate axis, if the upper segment of the line (the broken line in the figure) is extended backward.

This method of measurement is conformable to the definition given in Hungarian Standard MSZ 7980, according to which:

"By the term 'radial clearance' of the ring-oiling bearing is understood that distance which corresponds to a radial displacement of the inner race made in relation to the outer race, when the bearing is alternately subject to two equally large measurement loads operating in opposite radial directions, with regard to the most extreme positions." /27

In the case of an even number of balls and with a race displacement along an angle dividing line of the partial angle, the measurement result is equal to double the eccentricity, i.e., 2e. But if the number of balls is an odd number, the measurement result is equal to the sum e + h = e(1 + cos γ). /28
Naturally distortion of the shaft should be prevented during measurement.

2. Determination of Settling by Computation

Settling s, i.e., the displacement of the inner race measured in the direction of the normal force, is identical only in a mobile position with the oblateness δ of the ball found in the center of the load arc. On the other hand, in the case of a stable position the center of the load arc lies on the bipartition line of the angle between two neighboring balls, and this is at the same time the position of settling s; the value of s can be computed according to equation (3) from ball deformation and from the angle formed by the midline of the ball and the midline of the load arc. According to equation (4) the magnitude 2ζ of the load arc can be computed with a knowledge of settling s.

a) In the case of two load bearing balls the load of only one ball amounts to

$$N_1 = \frac{N}{2\cos\gamma}, \tag{18}$$

and the oblateness δ_1 of the ball according to the Hertzian equation [16] is

i.e.,

$$\delta_1 = 1{,}23\sqrt[3]{\left(\frac{N_1}{E}\right)^2 \frac{b/2+d/2}{b/2\cdot d/2}},$$

$$\delta_1 = s\cos\gamma = 1{,}23\sqrt[3]{\left(\frac{N_1}{E}\right)^2\frac{2}{b}\left(\frac{1+k}{k}\right)}, \tag{19}$$

where "b" = ball diameter;
+k = d/b = ratio of the inner race diameter to the ball diameter.

By introducing the above value of N_1 we get

$$\delta_1 = s\cos\gamma = 1{,}23\sqrt[3]{\left(\frac{N}{2\cos\gamma E}\right)^2\frac{2}{b}\left(\frac{1+k}{k}\right)}.$$

In the sense of equation (13) the load at any phase angle is

$$N = m\bar{n} = m\bar{a}\cos\varphi + m\bar{c} = P\cos\varphi + me\omega^2 = P\cos\varphi + C,$$

and therefore the oblateness at phase angle ϕ is: /29

$$\delta_1 = s\cos\gamma = 1{,}23\sqrt[3]{\left(\frac{P\cos\varphi + C}{2\cos\gamma E}\right)^2\frac{2}{b}\left(\frac{1+k}{k}\right)}. \tag{19a}$$

Maximum oblateness occurs at phase angle $\phi = 0°$ and is here

$$N_{max} = Q_{max} = P + C,$$

following which

$$\delta_{1max} = s\cos\gamma = 1{,}23\sqrt[3]{\left(\frac{Q_{max}}{2\cos\gamma E}\right)^2\frac{2}{b}\left(\frac{1+k}{k}\right)} \tag{19b}$$

and

$$s = \frac{1{,}23}{\cos\gamma}\sqrt[3]{\left(\frac{Q_{max}}{E\cos\gamma}\right)^2\frac{(1+k)}{2kb}}; \tag{20}$$

and in addition with any arbitrary angle ϕ and the normal force N coordinate to it, we get:

$$s_f = s\left(\frac{N}{Q_{max}}\right)^{2/3}. \tag{20a}$$

With a large number of revolutions the value of Q_{max} is to be modified in the sense of equation $\bar{e}' = e + s$, and according to equation (4) becomes

$$\cos\zeta_{max} = \frac{e + \cos\gamma}{e + \frac{1{,}23}{\cos\gamma}\sqrt[3]{\left(\frac{Q'_{max}}{E\cos\gamma}\right)^2\frac{1+k}{2kb}}}. \tag{21}$$

As long as the magnitude of the load arc ζ remains within the limits

$$\gamma < \zeta_{max} < 3\gamma$$

there are two load bearing balls.

But as soon as the value $\zeta_{max} > 3\gamma$ is reached, the load is borne by two pairs of balls.

b) The number of load bearing elements is any even number. In this case the computation procedure is formed somewhat differently from the process according to Stribeck for play-free roller bearings with an odd number of balls [1]. In a play-free condition the case of an odd number of bearing balls can also be valid as a stable condition; but if there is any clearance, in a "circling" movement the stable condition with an even number of bearing balls is much more probable and this is why the case of an even number of bearing balls is most obvious. /30

With several pairs of bearing balls, the deforming normal force is

$$N = 2(N_1 \cos\gamma + N_2 \cos 3\gamma + N_3 \cos 5\gamma + \ldots), \tag{22}$$

where the individual forces N_1, N_2, N_3... of the series designate the normal forces operating on the individual balls of each pair of balls.

With the value

$$\gamma = \frac{180^\circ}{z},$$

is valid according to (3)

$$\begin{aligned} \delta_1 &= s\cos\gamma, \\ \delta_2 &= s\cos 3\gamma, \\ \delta_3 &= s\cos 5\gamma, \\ &\ldots\ldots\ldots\ldots \end{aligned}$$

and

$$\begin{aligned} \frac{\delta_2}{\delta_1} &= \frac{\cos 3\gamma}{\cos\gamma}, \\ \frac{\delta_3}{\delta_1} &= \frac{\cos 5\gamma}{\cos\gamma}, \\ &\ldots\ldots\ldots\ldots \end{aligned}$$

In addition according to (19)

$$\begin{aligned} \frac{\delta_2}{\delta_1} &= \left(\frac{N_2}{N_1}\right)^{2/3}, \\ \frac{\delta_3}{\delta_1} &= \left(\frac{N_3}{N_1}\right)^{2/3}, \\ &\ldots\ldots\ldots\ldots \end{aligned}$$

is valid, and consequently

$$N_2 = N_1\left(\frac{\delta_2}{\delta_1}\right)^{3/2} = N_1\left(\frac{\cos 3\gamma}{\cos \gamma}\right)^{3/2},$$

$$N_3 = N_1\left(\frac{\delta_3}{\delta_1}\right)^{3/2} = N_1\left(\frac{\cos 5\gamma}{\cos \gamma}\right)^{3/2},$$

.....

from which

$$N = 2N_1\left[\cos\gamma + \left(\frac{\cos 3\gamma}{\cos \gamma}\right)^{3/2}\cos 3\gamma + \left(\frac{\cos 5\gamma}{\cos \gamma}\right)^{3/2}\cos 5\gamma + \ldots\right],$$

or

$$N = 2N_1\cos\gamma\left[1 + \left(\frac{\cos 3\gamma}{\cos \gamma}\right)^{5/2} + \left(\frac{\cos 5\gamma}{\cos \gamma}\right)^{5/2} + \ldots\right] \qquad (23)$$

/31

and therefore

$$N_1 = \frac{N}{2\cos\gamma\left[1 + \left(\frac{\cos 3\gamma}{\cos \gamma}\right)^{5/2} + \left(\frac{\cos 5\gamma}{\cos \gamma}\right)^{5/2} + \ldots + \left(\frac{\cos (2n-1)\gamma}{\cos \gamma}\right)^{5/2}\right.}. \qquad (24)$$

Thus with a knowledge of N_1 it is also possible to compute the ball load in other pairs of balls. By using an index n_g for n pairs of loaded balls and by introducing the designation "A_{ng}" for the polynomial between the brackets in the denominator of equation (24), we get

$$N_2 = \frac{N\left(\frac{\cos 3\gamma}{\cos \gamma}\right)^{3/2}}{2\cos\gamma A_{2g}}, \qquad (25)$$

for one outer ball with two pairs of bearing balls, and particularly in the case of $2n_g$ bearing balls the load of one outer ball (of the n_g-th pair) is

$$N_n = \frac{N\left[\frac{\cos (2n_g-1)\gamma}{\cos \gamma}\right]^{3/2}}{2\cos\gamma A_{ng}}, \qquad (26)$$

where the boundaries

$$(2n-1)\gamma < \zeta < (2n+1)\gamma$$

are fixed for the half load arc.

In order to find the angle ζ, it is sufficient to gradually compute the value of the load from one ball N_1 according to equation (24) for the increasing number of loaded pairs of balls, in order in this way to determine the coordinate value of ζ_{max} according to equations (20) and (21), and at the same time the number of effective load bearing pairs of balls. The criterion that the angle assumed in equation (24) coincides with that computed according to equation (21) is sufficient to show the correctness of the computation.

In order to simplify the computation, we have figured out individual values for

$$\frac{N}{N_1} = 2 \cos \gamma A_{ng} \tag{24a}$$

and are publishing these values for a series of z balls and n_g carrying pairs of balls in the following table:

TABLE OF VALUES OF A_{ng} AND N/N_1 AS FUNCTIONS OF NUMBER OF BALLS z AND NUMBER OF CARRYING PAIRS OF BALLS n_g (= $2n_g$ CARRYING BALLS): /32

The following designations form the basis of the computation of the values in the table:

$$A_{n_g} = \left[1 + \left(\frac{\cos 3\gamma}{\cos \gamma}\right)^{5/2} + \left(\frac{\cos 5\gamma}{\cos \gamma}\right)^{5/2} + \cdots + \left(\frac{\cos (2n-1)\gamma}{\cos \gamma}\right)^{5/2}\right];$$

N = the normal component of load Q which reaches the maximal value Q_{max} at $\phi = 0$;

N_1 = the load of one ball in the average pair of balls.

No. of Balls z	Half Partial Angle γ	No. of load bearers $2n_g$	Force Ratio N/N_1	Magnitude A_{n_g}	Half Load Arc ζ
6	30°	2	1.73	1	30°
9	20°	2	1.88	1	20°
		4	2.27	1.335	60°
10	18°	2	1.9	1	18°
		4	2.48	1.305	54°
12	15°	2	1.94	1	15°
		4	2.85	1.457	45°
		6	3.2	1.648	60°

TABLE (continued)

No. of Balls z	Half Partial Angle γ	No. of load Bearers $2n_g$	Force Ratio N/N_1	Magnitude A_{n_g}	Half Load Arc ζ
15	12°	2	1.96	1	12°
		4	3.18	1.623	36°
		6	3.54	1.807	60°
		8	3.55	1.810	84°
18	10°	2	1.97	1	10°
		4	3.42	1.735	30°
		6	4.33	2.196	50°
		8	4.47	2.267	70°
20	9°	2	1.976	1	9°
		4	3.5	1.777	27°
		6	4.38	2.214	45°
		8	4.65	2.355	63°
24	7° 30'	2	1.98	1	7° 30'
		4	3.65	1.842	22° 30'
		6	4.79	2.418	37° 30'
		8	5.38	2.717	52° 30'
		10	5.57	2.808	67° 30'
		12	5.58	2.814	82° 30'
30	6°	2	1.99	1	6°
		4	3.76	1.89	18°
		6	5.09	2.594	30°
		8	6.11	3.074	42°
		10	6.8	3.342	54°
		12	7.3	3.367	66°
		14	7.7	3.387	78°

The data of the above table are presented in Figure 10. Worthy of note is the circumstance that the average pair of balls in a bearing with few balls is loaded greater than in another bearing with more balls, viz., even with the same number of balls inside the load arc 2ζ. Thus, for example, when the load /33
inside the load arc is carried by six balls, the normal load force N_1, straining the average pair of balls, is equal to N/3.54 insofar as 15 balls operate in the bearing, while at z = 30 the ratio is N_1 = N/5.09. This is related to the magnitude of the load angle, at z = 15, 2ζ = 120°, while at z = 30 this angle is only 60°. In other words, load distribution is more uniform in a /34
bearing with more balls, because the angle of inclination of the outermost bearing balls to the normal force is smaller.

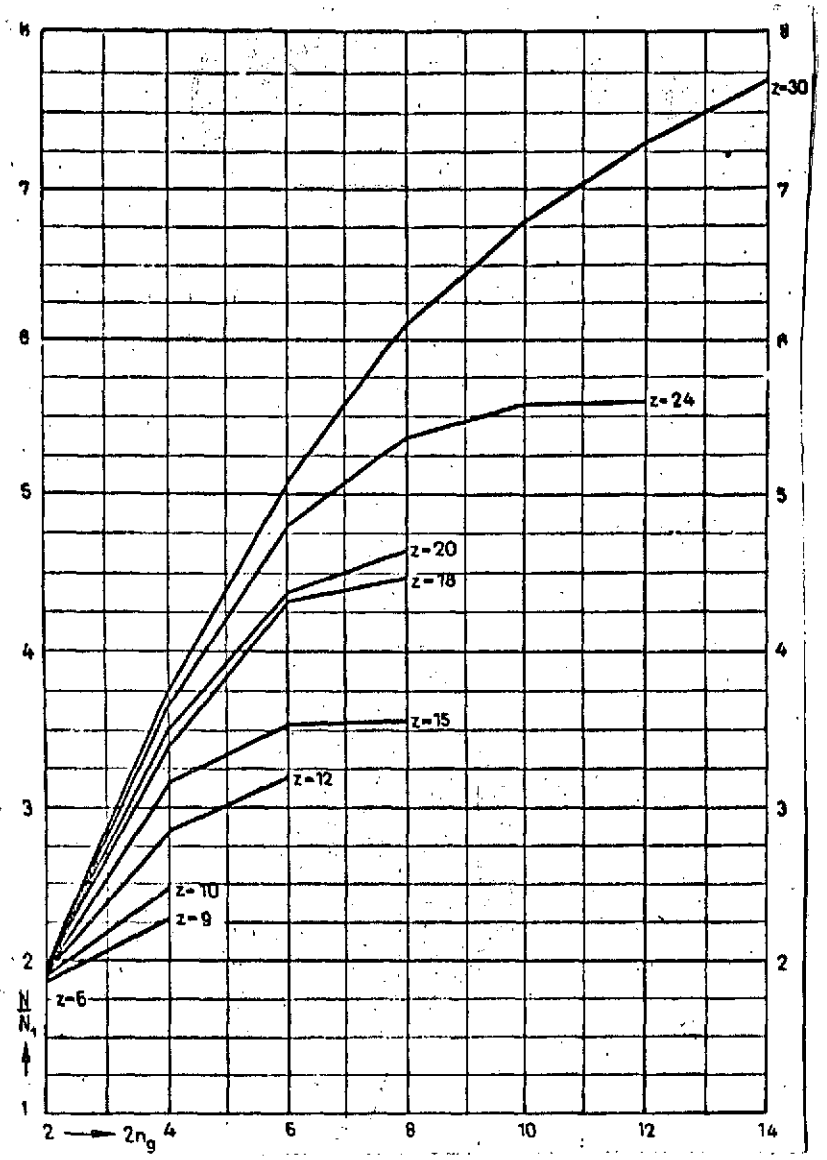

Figure 10. Ratio of the Normal Components of The Load To The Pressure On One Ball Of An Average Pair of Balls As A Function of The Number Of Bearing Balls With Different Total Numbers of Balls.

It will be demonstrated below that the magnitude of the load angle, not only in reference to load distribution, but also in respect to the expected vibration phenomenon, is an important factor.

VIII. THE IMAGINARY CIRCULAR REVOLUTION OF THE SHAFT MIDPOINT

From equation (20a) we get the value of settling s_i caused by the normal force N operating at any angle ϕ. If we imagine the case where the shaft midpoint O -- under compulsory operation (e.g., by a rocker arm rotating around point K) -- effectively describes the full circumference corresponding to the phase angle ϕ, where the normal force N freely exerts pressure on the mass point O, equation (20a) would be the correct formula for computing the circular revolution.

It is not difficult to describe this path geometrically. Namely, if we introduce the designation

$$\frac{Q_{max}}{N} = \nu$$

equation (20a) can be written in the following form:

$$s = s_i \nu^{2/3} = \text{const.} \tag{20b}$$

On the basis of the vector diagrams according to Figures 5a, 6a, 7a and 8a, the values ν can be constructively determined for every individual value of the angle of torsion ϕ plus the values s by means of the well-known Brauer procedure.

In this sense the auxiliary angle $\alpha = 45°$, assumed in Figure 11 on the basis of the equation

$$(1 + \tan\beta) = (1 + \tan\alpha)^{2/3}$$

is valid for angle β:

$$1 + \tan\beta = 2^{2/3} = 1.5874$$

and $\tan\beta = 0.5874$; $\beta = 30° 26'$.

Corresponding to the geometrical construction we have

$$\frac{s_1 - s_2}{s_2} = \tan\beta = \frac{s_1}{s_2} - 1,$$

and /35

$$\frac{\nu_2 - \nu_1}{\nu_1} = \tan\alpha = \frac{\nu_2}{\nu_1} - 1,$$

plus

$$\frac{s_1}{s_2} = 1 + \tan\beta = (1+\tan\alpha)^{2/3},$$

and

$$\frac{\nu_2}{\nu_1} = 1 + \tan\alpha,$$

from which it is clear that the geometric construction effectively corresponds to the conditions of equation [20b], because

$$\frac{s_1}{s_2} = \left(\frac{\nu_2}{\nu_1}\right)^{2/3},$$

i.e.,

$$s_1\nu_1^{2/3} = s_2\nu_2^{2/3} = \ldots = s = \text{const}.$$

If now a radius with the phase angle ϕ is drawn through point K and the distance s marked off on this radius in the direction of the normal acceleration $\bar{n}$ (measured from the point of the circumference with radius e), we get the points of the circular rotation (naturally the increasing movement in the direction of point K has a physical meaning only under the effect of a residual stress). Computation of a single value s is enough for geometric construction, because the acceleration values $\bar{n}$ can be taken from the vector diagram. /36

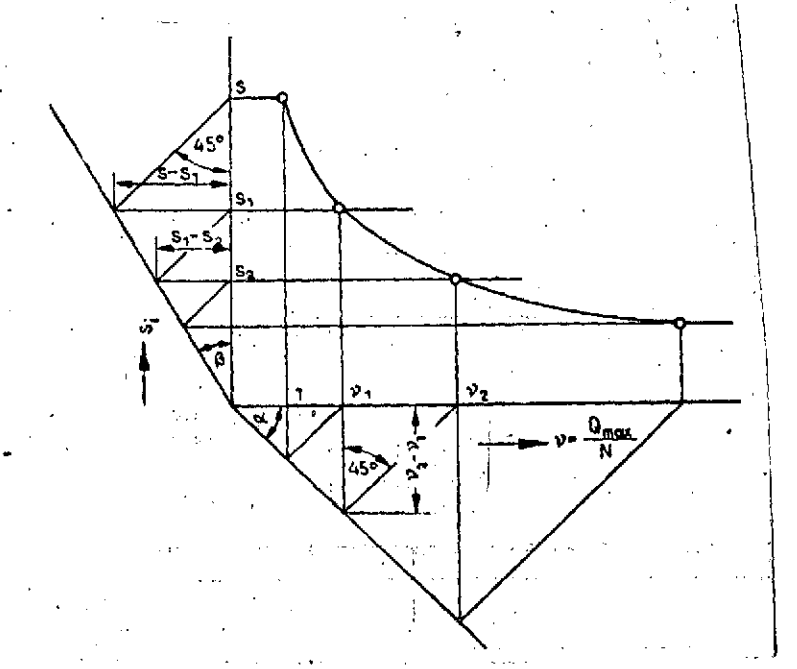

Figure 11. Constructive Determination Of The Rotational Path According to The Brauer Procedure.

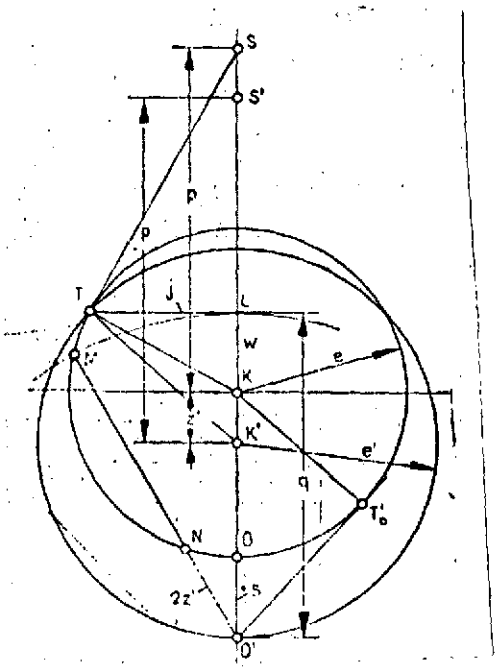

Figure 12. Protracted Circle For The Rotational Path (Points O' and T Are Elements Common to Both Circumferences).

However, it is superfluous to construct the circular path completely in this way. It will be shown below that the mass point O never follows this circular path: only a small arc sector is free for mass point O. Accordingly the theoretical circular path should be replaced by another circumference, namely of such a type that this replacement line completely follows the characteristic points of the theoretical line. In order to ascertain the vibrations of the shaft, we must determine the radius e' and the midpoint K' of this protracted circle with the mass of the pole distance p remaining unaltered, because according to equation (8) this magnitude depends only on acceleration $\overline{a}$, number of rotations n, and raceway diameters d and D, while the pole distance shifts on its own line into position K'S'.

Case 1. $\overline{a}/\overline{c} > 1$; $p > e$; Pole S at terminal

In Figure 12 we find the circle with midpoint K and radius e; this circumference is the rotational path without a load, i.e., without deformation. As initial data we here assume pole S, point of contact T of the tangents drawn from point S, and the settling s caused by the deformation occurring. Now the above defined protracted circle with its midpoint K' and diameter e' are to be determined in such a way that the circumference is to pass through point O' and the point of contact T: this assumption fulfills the above requirement according to which, in agreement with vector diagram 5a, maximum settling should amount to the mass s at point O' and deformation should disappear at point T. /37

The designations according to Figure 12 should now determine the unknown magnitude

$$KK' = z'$$

because the other unknown is already produced from it as

$$e' = e + s - z'$$

It follows from right angle LTK' that:

$$j^2 + (w + z')^2 = \overline{K'T}^2 = \overline{K'O'}^2 = (e + s - z')^2$$
$$j^2 + w^2 + 2wz'^2 + z'^2 = e^2 + 2es + s^2 - 2ez' - 2sz' + z'^2$$
$$2z'(w + e + s) = (e + s)^2 - (j^2 + w^2) ;$$

Now the figure shows the theorems: /38

$$j^2 + w^2 = e^2$$

and

$$w + e + s = q,$$

and thus

$$(e + s)^2 - e^2 = \overline{O'T'}^2,$$

and

$$2z'q = (e + s)^2 - e^2 = \overline{O'T'}^2,$$

are valid for the length of the tangents $O'T'_0$, and accordingly the simple construction process will take place as follows:

An arc is drawn with midpoint O' and radius q = O'L, and the point of intersection M of this circumference with the other circle of radius e is found, and in addition the point of intersection N is produced by drawing the line MO'. For this:

$$z' = \frac{O'N}{2},$$

is valid, and

$$z' = \frac{(e+s)^2 - e^2}{2q} = \frac{2es + s^2}{2(w+e+s)}, \qquad (27)$$

where, with reference to right triangle SKT:

$$w = \frac{e^2}{P}, \qquad (28)$$

and

$$e' = e + s - z'. \qquad (29)$$

The simple geometric consideration leads to the result that the midpoint K on line O'S is found by drawing the bisecting normals O'T as a point of intersection.

The protracted circle discussed remains as an overlapping line for the case of a high number of revolutions with small deformation. However, if the number of revolutions is small and deformation large, the protracted circle according to Figure 13 is useful. This circumference also passes point O and the tangent drawn from pole point S' touches the other circle of radius e at the same time.

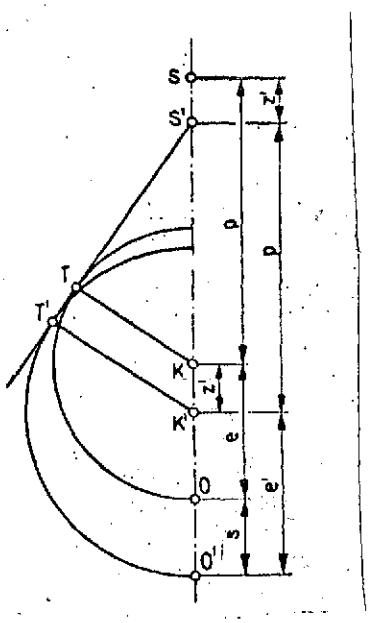

Figure 13. Protracted Circle to the Rotational Surface (Point O' and Tangent S'T' are Elements Common to Both Circumferences).

The deformation z', through which point K' is determined, can be ascertained as follows on the basis of the geometrical correlations: /39

$$S'O' : S'K' = S'O : S'K,$$

i.e.,

$$(s + e + p - z') : p = (e + p - z') : (p - z'),$$

and therefore

$$z'^2 - z'(p + e + s) + sp = 0.$$

Two circumferences pass through point O'; both are characterized by the tangents which are likewise drawn from point S' and touch the third circle (with radius e). We are interested in the one of these two variants whose result is the smaller z value, i.e.,

$$z' = \frac{(p+e+s) - \sqrt{(p+e+s)^2 - 4ps}}{2(p-e+s)}, \qquad (30)$$

and

$$e' = e + s - z',$$

where according to equation (30), when s = 0, z' also = 0, and e' becomes equal to e.

Case 2: $\bar{a}/\bar{c} > 1$; $p = \bar{a}/\omega_k^2 \to \infty$.

Here with $\phi = 0°$ and $\phi = 180°$ the absolute value of the normal force equals P both times; it follows from this that the circle whose radius is equal to eccentricity e can be displaced parallel to itself.

Case 3: $\overline{a/c} = 1$; $p = e$. The pole is on the rotational circumference

The radius of the protracted circle assumed to be at the position of the rotational curve and adjusted to it amounts to:

$$e' = \frac{2e + s}{2}, \tag{31}$$

where displacement amounts to:

$$z' = \frac{s}{2}. \tag{32}$$

But it is clear that this protracted circle cannot be accepted in the case where the value s is too large in relation to e. In regard to the invariable pole distance p, the radius of curvature of the rotational path at the upper zenith should be equal to "e". Thus the right path according to equation (20b) is produced.

Case 4: $\overline{a/c} < 1$; $p < e$ of pole S is within the circle of radius e /40

In such a case a distance s_{if} develops between the imaginary rotational path and the circle of radius e in the upper zenith also; for this equation (20a) produces:

$$s_{if} = s\left(\frac{P-C}{P+C}\right)^{2/3}$$

as a value of the deviation at the upper zenith point. From here we get

$$e' = \frac{2e+s+s_{if}}{2} \tag{33}$$

and in addition displacement of the rotational midpoint:

$$\overline{KK'} = z' = \frac{s-s_{if}}{2}. \tag{34}$$

It should also be pointed out that an acceptable protracted circle can be considered permissible in place of the imaginary rotational circumference because in general only a small arc sector takes a part in the vibration phenomenon.

NB: If the pole distance p is large, the circle of diameter

$$\overline{e'} = e + s$$

can be accepted as the protracted circle in the environment $\phi = 0$.

In order to preserve an absolutely consistent attitude, it should be noted here that the individual radii of curvature are obviously different on an oval rotational path. We know very well that the line of the pole distance must pass the midpoint of curvature; if we now analyze the displacement of midpoint K with the necessary theoretical severity, we must recognize that a deformation, which also changes under the effect of variable normal forces at different phase angles, may at times cause the formation of an oval rotational path, and it is also conceivable that the change in position of the pole distance can take place not only along its own straight line, but -- as a consequence of the nonuniformity of the radius of curvature of the rotational path, also as a displacement parallel to itself. Nevertheless the magnitude of the pole distance also remains unaltered in such cases. But we shall see that other vibrational movements can precede the phenomenon in question, and that a "jumping around" of the pole as a result of changes in the radius of curvature is probable only under great loads and at high rotational speeds.

IX. THE CONFIGURATION OF THE EFFECTIVE FORCES /41

From the discussions presented so far in reference to the rotation of a rotating system balanced exactly on its own axis in a roller bearing mounted with clearance, we have learned the following mechanical magnitudes which affect the shaft midpoint; the path in which the shaft midpoint circles under the effect of the deformation of the balls and the approximate circumference of the orbit mentioned.

Now we shall investigate what kind of movements results from the fact that /42
the effective forces likewise change when the angle of rotation is changed. Here we face two possibilities:

- Development of motions without regard for friction;
- Development of motions with consideration of friction.

Case 1: The pole distance is greater than the eccentricity.

$\overline{a/c} > 1$; $p > e$; Pole S at terminal distance.

In Figure 14a we see four bearing balls in the position $\phi = 0$, the corresponding half sector angle $\xi = 3\gamma$, where $e' = e + s - z'$, and we have a configuration in which the vectors of the outer balls A and B touch the circle of radius

$$\varrho' = e' \sin \xi \tag{35}$$

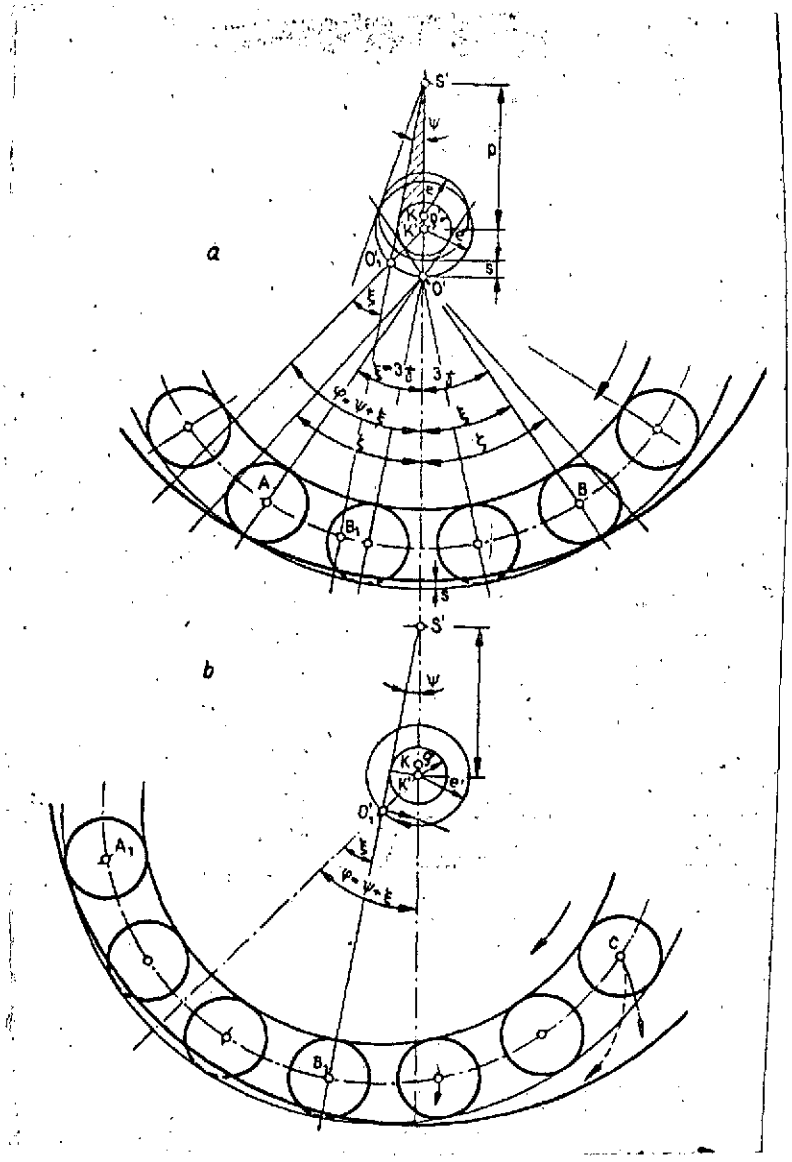

Figure 14. a) Load Bearing Group of Balls at $\phi = 0$ At Terminal Pole Distance. b) The Same Group in the Tilting Position When $\phi = \psi + \xi$.

During the rolling motion of the four bearing balls, shaft midpoint O' experiences a displacement along a path of eccentricity e'. It may happen that while shaft midpoint O' moves along the rotational path around point K' the normal component is reduced and therefore the two outer balls are loaded, as a consequence of which the base circle radius ρ' is also shortened now. The reason for this is that the magnitude of the base circle diameter depends greatly on the deformation caused by the load and on the number of the bearing balls.

On the presumption of a negligibly small load and with two balls in path contact, we get

$$\varrho' = e \sin \gamma . \qquad (35a)$$

In the sense of equation (35) the value ρ' increases proportionally to sin ξ, and at $2\xi = 180$, if the vectors of the outer bearing balls appear also as tangents of the circle of radius e', we get

$$\varrho'_{max} = e' \sin \frac{\pi}{2} = e'. \qquad (35b)$$

In the case presented in Figure 14a the following motion phenomenon are possible:

a) While the inner race rolls on the four bearing balls, the shaft midpoint O' describes a circular motion along a circle of radius e' until finally, in the given direction of rotation, the vector of the "last" bearing ball "B" /43

passes the force midpoint S'. This new position B_1 of the ball can be found in the following way:

A tangent is drawn from point S' to the base circle (of radius ρ'). This line intersects the midcircumference of the ball rim in the new point B_1 and the same straight tangent intersects the eccentricity circle (of radius e') in the new shaft midpoint O'_1.

Figure 4b shows the new configuration in which balls A and B accept their new positions A_1 and B_1. We see that not all four balls can continue to be loaded, since now the "last B" ball leaves the operating line $S'O'_1$ of the force, and finally the ball "tilts" around point B_1 from its position in O'_1, i.e., "backwards". In this way the entire ball rim performs a tilting motion, that is of such a sort that ball C of the next group of four describes an arc sector with midpoint B_1 at the beginning of tilting, but ball C immediately leaves this path because ball B in the meantime is forced to change its position. Tilting of the shaft midpoint O'_1 also begins along an arc, but this movement also suffers an alteration, likewise because of the effect of the forward motion of tilting center B. In any case it can be determined that after the end of the tilting motion the shaft midpoint O again assumes its position on the eccentricity curve of radius e'.

The initial position of the tilt motion can also be simply computed in the following way:

According to the designations of Figure 14b the theorems

$$\varphi = \psi + \xi \tag{36}$$

and

$$\varrho' = p \sin \psi . \tag{37}$$

exist for the triangle $S'K'O'_1$. From these formulae it is possible to deduce the angle ψ in order to determine the angle of torque ϕ (see equations (8) and (35)):

$$\sin \psi = \frac{\varrho'}{p} = \frac{(e+s-z') \sin \xi n^2}{91\, a} \left(\frac{d}{D+d} \right)^2 . \tag{38}$$

Equation (19a) is suited for recognizing whether the balls with a given load are unloaded during torque. After all, if the reduction in load leads to unloading balls, the following phenomena are involved (according to equation

(38)): as a result of the reduction s angle ψ is reduced, and suddenly angle ξ also, causing the phase angle ϕ to become smaller, which means that the tilting occurs even earlier, i.e., before the midposition is reached.

After tilting the shaft midpoint recovers its circular orbit on the path of radius e'. /44

b) A load case can occur in which the half sector angle ξ of the bearing ball is almost equal to 90°, and thus it happens that the "last" bearing ball can no longer leave the operating line of the pressure during the circling motion of the shaft midpoint O'. In such a case, as already mentioned, the base circle radius ρ' is nearly equal to the eccentricity radius e', and therefore no tilting can occur under such a load.

From the literature [19] we learn that in a friction bearing with clearance, during rotation, the shaft midpoint relative to the rest position describes a "circling motion" in the direction opposed to the rotation, at which time the tangential component of the effective force is equal to the frictional force [20]. On the other hand in a roller bearing with clearance the torque of the shaft midpoint under the effect of rolling is equal to the direction of rotation, leading to a "rocking" motion when it has a vibrating load.

In those cases of load in which "tilting" can occur, the forward slip mentioned has an influence on the beginning of tilting or may at the same time cause rocking.

On the basis of equations (13) and (14) angle $\bar{\phi}$, at which backward rocking occurs, can be computed; for this purpose the value of the coefficients of friction μ between balls and path should be accepted as a symbolic magnitude and at the same time as a basis for comparison (Section XI contains an exhaustive discussion of this matter).

At the moment when

$$\mu N < T,$$

the shaft midpoint can rotate backward, and thus the limiting case is described by the designation

$$\mu m (\bar{a} \cos \bar{\varphi} + e' \omega_k^2) = m\bar{a} \sin \bar{\varphi},$$

or by

$$\bar{a} \sin \bar{\varphi} - \mu \bar{a} \cos \bar{\varphi} = \mu e' \omega_k^2,$$

or expressed by

$$\frac{\sin \bar{\varphi} - \mu \cos \bar{\varphi}}{\mu} = \frac{e' \omega_k^2}{\bar{a}}$$

With consideration of equation (8) after the introduction of the frictional angle $\bar{\rho}$, i.e., after introducing the statement $\mu = \tan \bar{\rho}$, we get

$$\frac{\sin \bar{\varphi} \cos \bar{\varrho} - \cos \bar{\varphi} \sin \bar{\varrho}}{\sin \bar{\varrho}} = \frac{\sin (\bar{\varphi} - \bar{\varrho})}{\sin \bar{\varrho}} = \frac{e' \omega_k^2}{\bar{a}} = \frac{e'}{p}. \tag{39}$$

From this it follows that in our case $\bar{\phi} - \bar{\rho} < \bar{\rho}$, or /45

$$\bar{\phi} < 2\bar{\rho}$$

and in consideration of equation (7) we get the formula for determining $\bar{\phi}$:

$$\sin (\bar{\varphi} - \bar{\varrho}) = \frac{\sin \bar{\varrho}}{91} \frac{e'}{\bar{a}} n^2 \left(\frac{d}{D+d} \right)^2, \tag{39a}$$

for which we get the value e' from equation (20) and the value z' either from equation (27) or from equation (30).

Worthy of note is the phenomenon which was observed in connection with friction bearings of low revolution [11]: under certain conditions jerky motions "backwards" also occur here, and often cause disruptive vibrations.

Case 2: The force midpoint in infinity; $\bar{a}/\bar{c} > 1$; $p = \bar{a}/\omega_k^2 \to \infty$.

If under certain conditions relating to load the number of revolutions is very low, this is a special variation of the case under preceeding point 1. A pole position in infinity has the physical meaning that the force vector follows along parallel to the shaft midpoint O into every new position.

a) Figure 15 shows two load bearing balls, and thus the half angle of load amounts to $\xi = \gamma$. The straight lines which are drawn from the pole point $S \equiv S'$ in infinity as tangents to the circle of radius e can only touch the other circle around midpoint K of radius e' if the original eccentricity circle is displaced parallel to itself along the settling distance s in the direction of the force vector P. The shaft midpoint displaced into position O' as the result of deformation will only circle the loaded ball B as long as this ball, along with the shaft midpoint, reaches the operating line of force P or overtakes it. With the position of the shaft midpoint at O'_1 and with the ball in position B_1 (in the designated direction of rotation) the entire ball rim and also the shaft undergo tilting at B_1. After the tilting, if ball A moves into the new position A_1, the vector of this ball no longer appears as the tangent of the base circle (of radius ρ'). Instead of this vector we find the one of ball B_1 and instead of the vector of B, we find that of ball C,

which now adopts position C_1 as a bearing ball (Figure 15a). Since ball C suffers deformation immediately after tilting also, the displacements occurring are not designated by the half load arc ζ, but by the half load angle ξ.

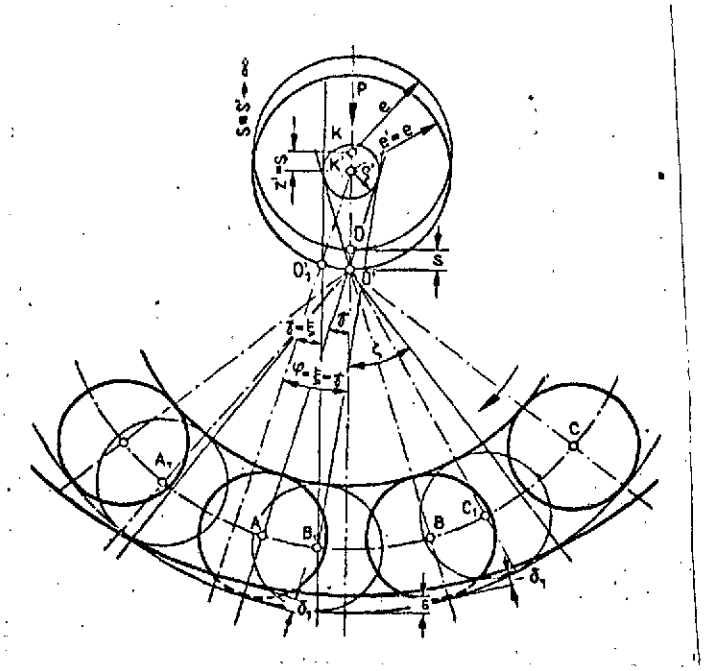

Figure 15. Midposition of a Bearing Pair of Balls (ϕ = 0), And Its Tilt Position (ϕ = γ) At An Infinite Pole Distance.

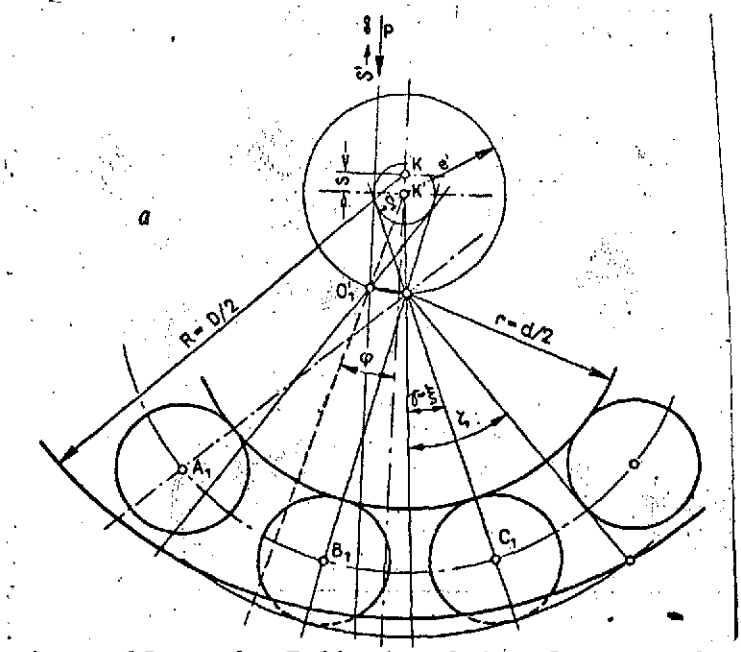

Figure 15a. The Following Pair of Balls After the Change.

Since under such operational conditions /47

$$\psi = 0$$

the phase angle according to equation (36) in the first moment of starting of tilting is:

$$\phi = \xi. \tag{40}$$

b) We can compute the angle $\bar{\phi}$, at which the back rocking begins, from a knowledge of the angle of friction ρ, of the normal acceleration n (according to 13a) and of tangential acceleration (the expression of which according to (14) also remains valid for this case). Now

$$\mu \bar{n} \leq \bar{t}$$

and in the limiting case

$$\mu \bar{a} \cos \bar{\varphi} = \bar{a} \sin \bar{\varphi},$$

i.e.,

$$\tan \bar{\varphi} = \mu = \tan \bar{\varrho}$$

and

$$\bar{\phi} = \bar{\rho}. \tag{41}$$

Case 3: $\bar{a}/\bar{c} = 1$; p = e, Pole S lies on the rotational path.

In Figure 16 only the following geometrical magnitudes are presented: for the case without deformation the rotational path of radius "e"; for the case of deformation, thus with a changed rotational path (which however is not drawn in the figure), the protracted circle of radius e', which circle sticks /48
both to the rotational path mentioned and to the rotational path changed, the base circle of radius ρ'.

a) The magnitude of the phase angle ϕ at the moment tilting begins can be determined by simple consideration of triangle $S'K'O'_1$ with the same legs; here the following equations are valid:

$$\xi = \psi;$$

$$\rho' = e' \sin \psi = e' \sin \xi, \tag{42}$$

and the following is valid for the mentioned value of the phase angle

$$\phi = 2\xi. \tag{43}$$

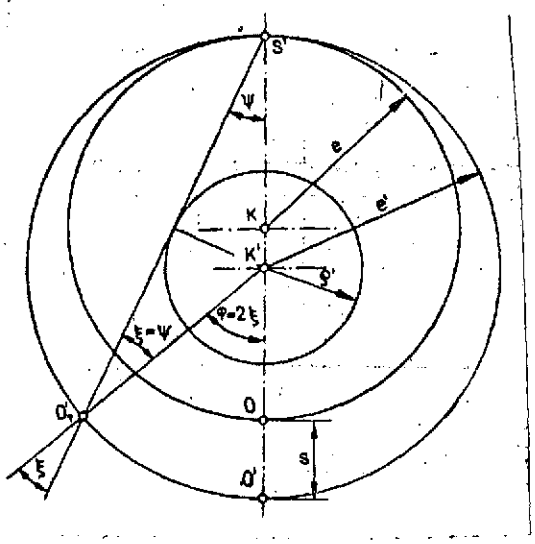

Figure 16. Rotational Path, $\phi = \psi$. (Pole on the Rotational Path).

b) In order to determine the phase angle at the moment backward vibration begins, equations (16) and (14) are also valid this time, i.e.

$$\mu \bar{a} (1 + \cos \bar{\varphi}) = \bar{a} \sin \bar{\varphi},$$

or

$$\frac{\sin \bar{\varphi} - \mu \cos \bar{\varphi}}{\mu} = 1.$$

With the well-known definition

$$\mu = \tan \bar{\varrho}$$

we get

$$\frac{\sin \bar{\varphi} \cos \bar{\varrho} - \cos \bar{\varphi} \sin \bar{\varrho}}{\sin \bar{\varrho}} = 1$$

and additionally

$$\sin (\bar{\varphi} - \bar{\varrho}) = \sin \bar{\varrho},$$

i.e.,

$$\bar{\varphi} = 2\bar{\varrho}.$$

Case 4: $\overline{a/c} < 1$; $p < e$. Pole S lies within the rotational path of radius e.

In this section in speaking about the first three cases we have followed the procedure where the force midpoint S beginning from its position in infinity moves inward until the eccentricity circle is finally reached. But it is much more complex to accurately observe the phenomena when the pole accepts the position within the eccentricity circle (of radius e) or even within the base circle (of radius ρ'). Precisely in these cases the operating considerations require the most exact determinations, the importance of which must be particularly underscored because of the heating to be expected in the high revolution area and because of the emphasized need for a well founded bearing clearance. /49

It may appear strange that the last tenths of millimeters on the path of the "wandering" pole must be found with tedious deliberation as the stretch from the position (corresponding to the so-called zero revolution) infinitely inward to the eccentricity circle. But we must not forget how extreme requirements are on surface properties and how narrowly the involved tolerance ranges are measured, for which the prescribed figures shift by a few μm, in contradistinction to which radial bearing clearance, even for roller bearings of average size, may reach a mass of 1/10 mm [14], thus sometimes 100 times greater than the irregularities of the surface. We cannot avoid a comparison

with a cross-country vehicle called upon to master ditches of 8-10 meters depth in addition to clods of earth about 8-10 cm in size.

a) With an unchanged load, but with increasing revolutions, the pole S approaches midpoint K, a prerequisite of tilting (Figure 17) is

$$\phi = \xi + \psi$$

where the value of ϕ can be ascertained from equations (21), (35) and (37). In the three cases discussed above a position could always be found in which the normal component of the load Q became zero (see Figures 5c, 6b, 7b). Now in the previous case (Figure 8b) the normal force components never disappeared, and therefore the question rises as to whether a limiting position could be found in which the condition described above as necessary for causing tilting is not sufficient. We shall now prove that such a position actually does occur if the pole point just reaches the range of the base circle (of radius ρ'). /50

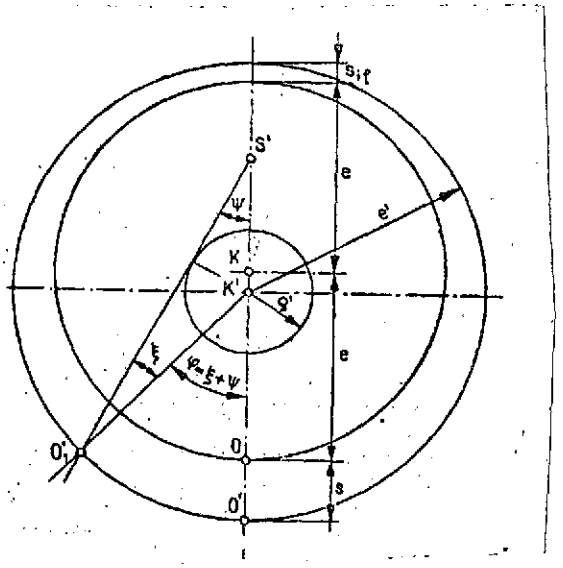

Figure 17. Rotational Path (Pole Inside The Rotational Path).

In Figure 18 we have presented the load bearing group of balls in the position at which the shaft midpoint is found at point O', when at the same time with ball B functioning momentarily as a tilting point, the distance BN is assigned as a momentary spoke to the outer force P and the distance BN to the centrifugal force. In the course of continual rotational movement the spoke of the centrifugal force remains unchanged, but the spoke of power P keeps increasing and reaches its highest value in the position of B_ρ when radius $O'_\rho B'_\rho$ forms a right angle with force P.

If now the largest movement of force P is still smaller than the moment of the centrifugal force, no tilting can occur. In this position the momentary equilibrium can be expressed as follows with the designations of Figure 18:

$$PR_k = CR_k \sin \xi.$$

Since now

$$P = m \cdot \bar{a}$$

and

$$C = me' \omega_k^2 = me' \frac{n^2}{91} \left(\frac{d}{D+d}\right)^2,$$

we can determine the limiting number of revolutions n_h at which tilting can no longer occur; the equation is then:

$$n_h = 9{,}55\left(\frac{D+d}{d}\right)\sqrt{\frac{\bar{a}}{e'\sin\xi}} = 9{,}55\,\frac{D+d}{d}\sqrt{\frac{\bar{a}}{\varrho'}}\,. \qquad (45)$$

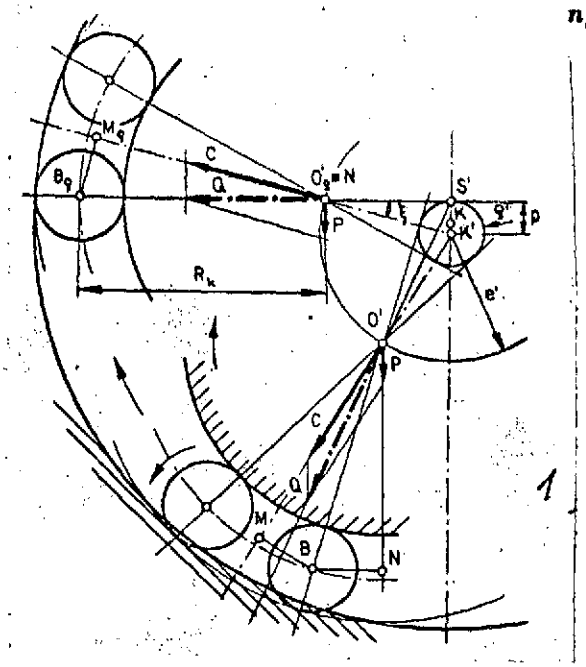

Figure 18. Case of Limiting Revolutions (Pole on Circumferences of Base Circle of Radius ρ').

In agreement with equation (8), the critical number of revolutions occurs in the event that

$$P = \rho'.$$

But now the value ρ' obviously increases with the number of balls, and respectively to deformation, in the sense of the equation

$$\rho' = e' \sin \xi. \qquad (46)$$

In other words a larger deformation is related to a drop in the limiting number of revolutions.

b) The normal force and the tangential force are also expressed by equations (13) and (14) in agreement with case 1. Only then we have $\bar{a}/\bar{c} > 1$ and here $\bar{a}/\bar{c} < 1$ is valid.

According to equation (39) we can write:

$$\frac{\sin(\bar{\varphi}-\bar{\varrho})}{\sin\bar{\varrho}} = \frac{e'}{p} > 1,$$

from which it follows that

$$\bar{\varphi} > 2\bar{\varrho}. \qquad (47)$$

We wish now to consider the case of $p = \rho'$ in more detail; with equations (35) and (39) we have for this case:

$$\frac{\sin(\bar{\varphi}-\bar{\varrho})}{\sin\bar{\varrho}} = \frac{e'}{p} = \frac{\varrho'}{p\sin\xi} = \frac{1}{\sin\xi}.$$

Angle ξ moves between γ and 90°, i.e., /52

$$\sin(\bar{\varphi}-\bar{\varrho}) = \sin\bar{\varrho} \ldots \frac{\sin\bar{\varrho}}{\sin\gamma}.$$

In the limiting case of $\xi = 90°$, $\bar{\phi} = 2\bar{\rho}$ is thus in agreement with (44), since when $\xi = 90°$ we have $e' = \rho'$ (according to equation 35) at the same time. When we have the limiting case $\xi = \gamma$ before us, $\bar{\phi}$ can be unambiguously determined, where this $\bar{\phi}$ value (according to equation 47) is greater than $2\bar{\rho}$. This is unmistakenly related to the fact that as p continues to drop the occurrence of a peripheral movement becomes more and more probable.

In a roller bearing with clearance we have discovered three kinds of vibrational movement possible for the rotating mass balanced on its own axis: tilting, rocking and, in case the pole is shifted inside the base circle, peripheral movement. But up to now we had not said anything in detail about this third phenomenon. In Section XI we shall decide the question of whether balls roll or slide in this movement.

X. THE VIBRATION PATH

1. The Rocking Angle

If the roller bearing works only under a moderate radial load or must transmit only a torque moment, deformation is negligibly small, and therefore the base circle radius (Figures 1 and 2) amounts to

$$\rho = e \sin\gamma = h \tan\gamma = p \sin\phi.$$

If we disregard friction, rocking vibration cannot occur and a tilting action takes place only until pole point S reaches the base circle (of radius ρ) as a result of an increase in revolutions. It can be determined by direct geometrical consideration that a tilting motion cannot occur once the pole distance is smaller than the base circle radius, namely because the tilting position geometrically represents that tangent which is drawn from pole point S to the base circle (of radius ρ). There are no tangents from a point which lies within the circle.

As soon as we are concerned with a radial load, deformation must also be taken into consideration. In this connection it was necessary to introduce another, i.e., a protracted circle of radius e' to replace the rotational path of radius e, but here the radius of the base circle became greater than the original value, namely

$$\rho' = e' \sin\xi$$

Here ξ with a small load can even be equal to γ, and with a greater load is $\xi \approx 180°/2$, and therefore: /53

$$\rho'_{max} \approx e'.$$

When the concept of friction is brought in, we must deal with the phenomenon of rocking vibrations, characterized by the rocking angle $\overline{\phi}$. The meaning of this is that the tilting position is no longer actually identical to that determined geometrically, but is displaced around the rocking angle. As already mentioned, this angle depends upon the pole position. While the pole position works its way inward from infinity to the rotational path of the shaft midpoint, angle $\overline{\phi}$ climbs from its initial value $\overline{\rho}$ to the value of $2\overline{\rho}$. If the pole distance is shortened even more, the value of the rocking angle increases more.

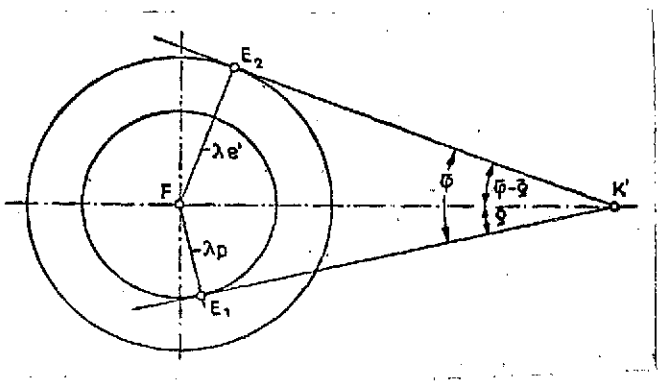

Figure 19. Relationship Between The Angle of Friction and the Rocking Angle With Pole Distances of Different Magnitude.

The geometric clarification of equation (39) is presented in Figure 19. The tip of the angle $\overline{\rho}$ lies at point K'. On one of the legs we choose any point F as the midpoint of a circle which, with radius FE_1, touches the other leg at point E_1. Now we construct a second circle of radius FE_2 concentric to the first circle, with the ratio of the radii mentioned corresponding to the following equation

$$\frac{FE_1}{FE_2} = \frac{\gamma\rho}{\gamma e'} = \frac{P}{e'}$$

If we now draw a tangent from point K' to this second circle, we get the rocking angle:

$$E_1K'E_2 = \overline{\phi}.$$

In Figure 20 we see the geometrical construction of the rocking angle $\overline{\phi}$ in a roller bearing. From point S' to the circle (with radius ρ') is drawn a tangent whose point of intersection with the circle (of radius e') lies at O'_1, with the point of intersection with the external rolling circle lying at B_1. This tangent characterizes the tilting position without friction. In

this position $K'O_1'$ is the midline of the bearing group of balls. This midline intersects the outer rolling circle at point E_1. Now the circle of radii FE_1 and FE_2 are constructed from point F on the other leg of the angle $\bar{\rho}$ in such a way that the following equations are valid for the segments:

$$FE_1 = K' E_1'$$

and

$$FE_2 = K' E_2'$$

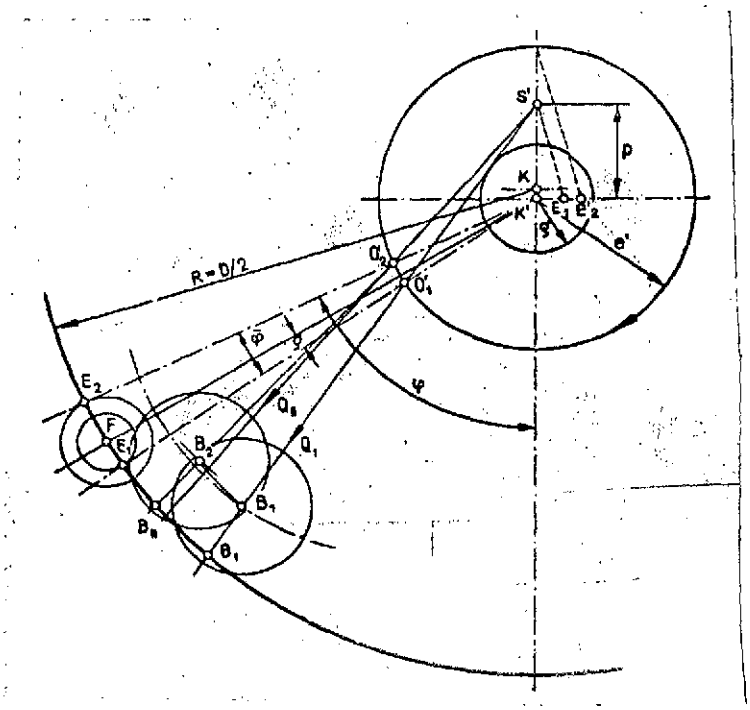

Figure 20. Determination of the Phase Angle of the Rocking Motion.

In the geometrical construction we see the two parallel lines by means of which

$K' E_2' : K' E_1' = e' : p$

would correspond to the ratio.

The straight line $K' E_2$ intersects point O_2' outside the circle (of diameter e'). /55

Now $K' O_2'$ is the midline of the bearing group of balls in the new tilting position. The rocking angle is

$$\sphericalangle E_1 K' E_2 = \sphericalangle O_1' K' O_2' = \bar{\varphi}.$$

In order to find the new point of contact B_{11} of ball B on the outer course, it is enough to make the uniformity of the segments valid, as follows (Figure 20):

$$E_2 B_{11} = E_1 B_1.$$

In addition the picture shows that the operating line of force Q_1, which originating from pole S' passes the mass point O_1', also strikes the ball

midpoint B_1. The force line operating on line $S'O_2'$ cannot, however, not strike the ball midpoint of ball B_2, and therefore the ensuing torque moment holds a balance at the time with the frictional moment.

The theorem that the direction of development of the rocking angle is identical to the direction of torque of the shaft can be decided by simple consideration of Figure 18 on the basis of the guide arrows inscribed (in individual hatched surfaces in the diagram).

2. Tilting Path

Within the space conditioned by bearing clearance, the most characteristic motion of the possible displacements of the shaft of the roller bearing is tilting, since this must be dealt with whether deformation occurs or not, and regardless of whether there is a lower or higher number of revolutions. If we prescind from the rocking motion and limit ourselves to describing tilting alone, the computational results still remain quite involved and hard to summarize, being a consequence of the extremely great variability of the curves along the path of the tilting sector of this vibration phenomenon in connection with the multiple differentiation in operating parameters.

The question could be formulized in such a way that the path of the individual mass point O of a weightless rod is to be described if a point B of this rod moves along a circle of radius R with an angular velocity ω_k and with an unaltered position of the force midpoint S' (Figure 21).

With a small load and two bearing balls $\xi = \gamma$; in such a position, and especially at the beginning of tilting, we get according to (36)

$$\phi = \psi + \xi.$$

After the "tilting segment" OFO_1 has run its course, the "drag segment" O_1GO /56
follows along the circle (of radius e') as a conclusion of the vibration path. If we consider the tilting center B as immobile for the length of the tilting, we can observe the following relationship:

The radial or zenith amplitude

$$OO_1 = y$$

is found at a right angle to the tangential or thrust amplitude

$$FG = X$$

of the closed vibration path. Now the zenith point F of this amplitude will appear in that position of point B if point O stands in opposition to both points B and K'. In Figure 23 the displacement of the tilting midpoint was also taken into consideration.

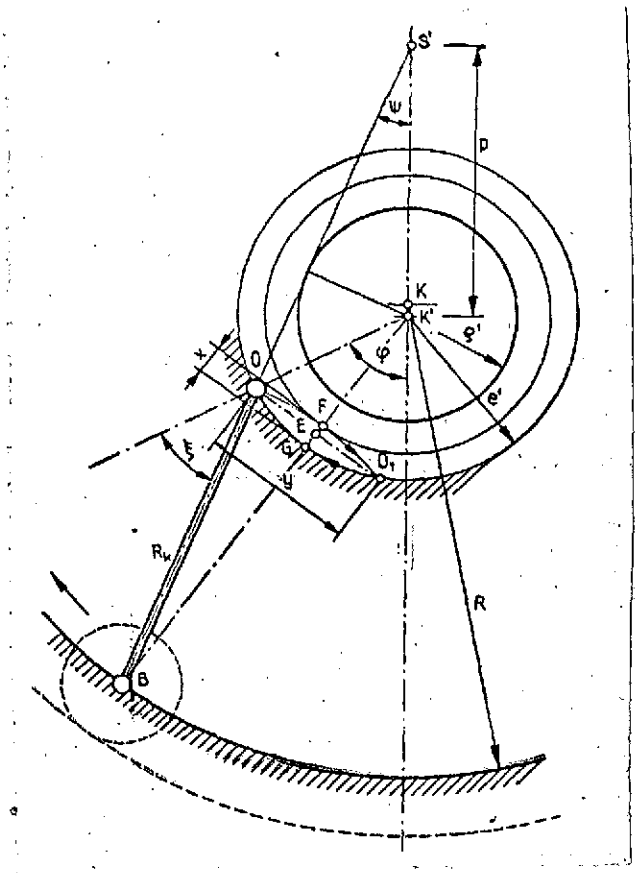

Figure 21. The Path of The Tilting Motion.

The phase angle ϕ at the beginning of the tilting process can be accurately determined according to equations (36) and (38).

However, the position of the force midpoint S' likewise remains unchanged with an unchanged load and constant revolution, and consequently the measurement of the "tilting segment" OFO_1 is constantly repeated in the same magnitude, even if another bearing group of balls enters the position of the previous ones; in other words the rapidly successive hammering forces strike the same spot on the race; it is imaginable that we can perceive here

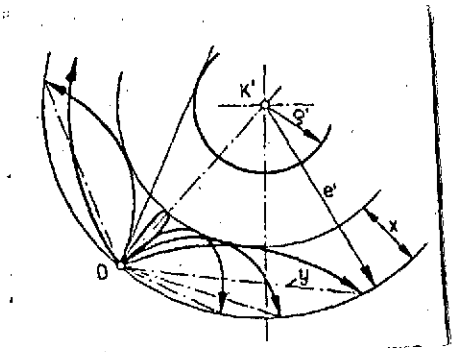

Figure 22. Tilting Curves, Referred to Their Common Point of Origin.

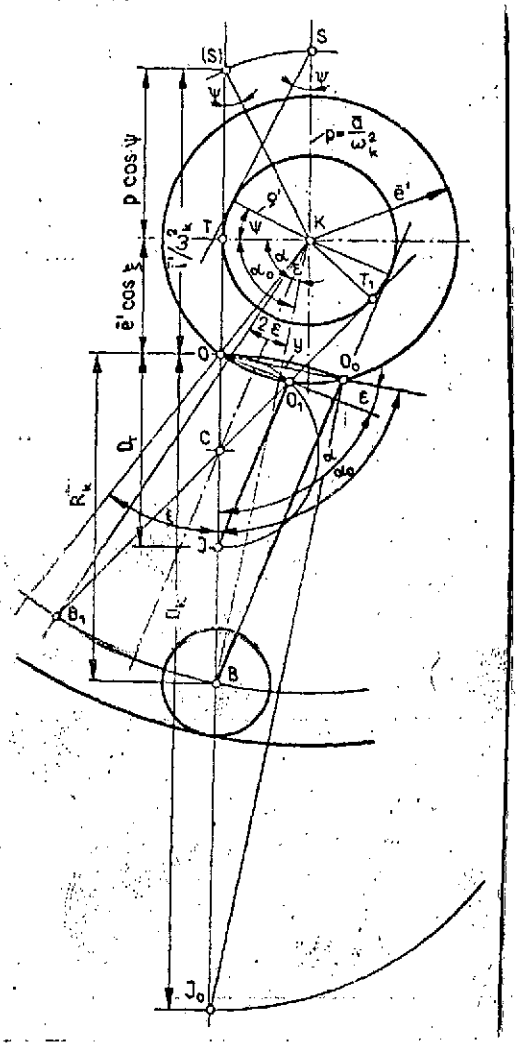

Figure 23. The Sloping Line in the Thales Circle For Dealing With Thrust Amplitudes.

/57

the cause of the so-called "flaking", without bothering about whether the deformation (with a small load) is negligible or whether we have to deal with deformation.

With a small angular velocity of ball B we can look at the tilting segment as an arc of midpoint B; however, if the angular velocity ω_k becomes greater (i.e., if the pole distance p is diminished), the amplitude y will diminish in the beginning and then completely disappear. If the value of ω_k increases again, the amplitude y will return in the other direction and will keep growing until the circling movement finally occurs in place of the tilting.

In the beginning amplitude x retains its size, even if y becomes zero; when y changes direction, x gradually becomes smaller and when circling movement begins it approaches the zero value.

In Figure 22 we see the tilting curves developed at various phase angles, but initial point O is centralized in them (by twisting around point K'). In the sense of this figure the amplitude x should be designated as "zenith amplitude", and the amplitude y as "thrust amplitude".

3. Approximate Computation of Thrust Amplitude

Let us now imagine a configuration of forces which operate at the initial points of the tilting motions occurring at various phase angles, presented in such a way that these force vectors come to lie on a single line around point K. In this figure, where every force Q is thus oriented in the same SO direction, the pertinent thrust amplitude appears as an oblique line with a certain angle of inclination α. This kind of presentation can be seen in Figure 23, in which the turning of the force vectors mentioned above was made in the operating line of every tilting force which is effective at pole point S lying in infinity. The angle of torque is equal to the angle ψ coordinated for the pole in question. For the sake of simplicity we have shifted the midpoint of the circle of radius $\bar{e}'$ in this picture to point K. /58 /59

If we first assume a pole point S lying in infinity, and then imagine point B during tilting as stationary, the time which corresponds to the oblique segment OO_0 as the path traveled will correspond to the time period which would be necessary to cover a distance equal to the diameter ($D_k = OJ_0$) of the Thales Circle by free fall with the operation of acceleration proceeding from point S. Now, however in the case of a pole distance of finite magnitude, the value of ω_k is far from zero, and the tilting point B is therefore not stationary: consequently the "thrust amplitude" becomes smaller and the time period of the "tilting segment" becomes shorter, that is in comparison to the case of an infinite pole distance. The geometric solution can be found if there is success, for any value of the pole distance, in determining the diameter of the pertinent Thales circle and the angle of inclination α.

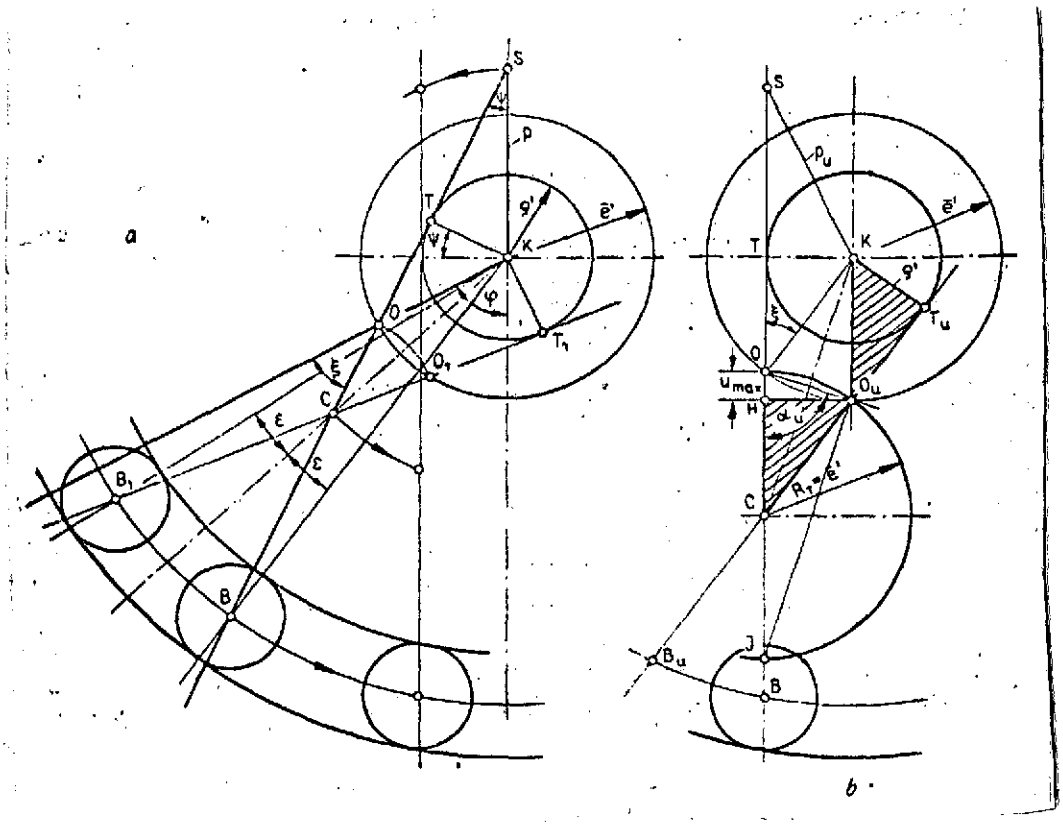

Figure 23a. Generation of Thrust Amplitude With A Shift In The Tilting Center.
Figure 23b. Configuration With Maximum Dynamic Effect

According to Figure 23a and proceeding from any pole distance the angle corresponds to /60

$$\sphericalangle BKB_1 = 2\varepsilon = \omega_k t,$$

of the torque made by the ball as the tilting midpoint during tilting time t relative to the specific tilting arc radius $\overline{BK}$. This comes from the circumstance that the vector of the ball touches the circle of radius ρ' at the beginning of tilting at point T and at the end of tilting at point T_1.

Likewise according to Figure 23 the following formula is valid for the angles with any perpendicular leg

$$\sphericalangle BKC = \sphericalangle O_0 OO_1 = \varepsilon = \alpha_0 - \alpha.$$

Now we must determine the path of a free fall which can be covered with the operation of a tilting acceleration $\bar{i}'$ coordinated with a given pole distance during the time of

$$t = \frac{2\varepsilon}{\omega_k}$$

just because this path segment will be equal to the diameter $D_T = OJ$ of the Thales circle coordinated to the given pole distance. In this sense we have

$$t = \sqrt{\frac{2D_T}{\bar{i}'}} = \frac{2\varepsilon}{\omega_k} = \frac{2(\alpha_0 - \alpha)}{\omega_k}$$

and

$$D_T = \frac{2\bar{i}'(\alpha_0 - \alpha)^2}{\omega_k^2}. \tag{48}$$

However now the right triangle KTC produces:

$$CT = \frac{D_T}{2} + \bar{e}' \cos\xi = \varrho' \tan\alpha,$$

and also

$$D_T = 2\varrho' \tan\alpha - 2\bar{e}' \cos\xi. \tag{49}$$

In addition with

$$\rho' = \bar{e}' \sin\xi$$

and from equations (48) and (49) we have:

$$\frac{\bar{i}'}{\omega_k^2}(\alpha_0 - \alpha)^2 = \varrho' \tan\alpha - \bar{e}' \cos\xi = \bar{e}' \sin\xi \tan\alpha - \bar{e}' \cos\xi,$$

from which follows the goniometric equation helping to determine α:

$$\alpha^2 - 2\alpha\alpha_0 - \frac{\omega_k^2}{\bar{i}'}\bar{e}' \sin\xi \tan\alpha + \frac{\omega_k^2}{\bar{i}'}\bar{e}' \cos\xi + \alpha_0^2 = 0. \tag{50}$$

With the first two members of the series /61

$$\tan\alpha = \alpha + \frac{\alpha^3}{3} + \frac{2}{3}\frac{\alpha^5}{5} + \frac{17\alpha^7}{3^2 \cdot 5 \cdot 7} + \dots$$

is produced the third degree equation

$$\alpha^3 - \frac{3\bar{i}'\alpha^2}{\omega_k \varrho'} + \left(\frac{6\alpha_0}{\varrho'}\frac{\bar{i}'}{\omega_k^2} + 3\right)\alpha - \left(\frac{3\bar{e}'}{\varrho'}\cos\xi + \frac{3\alpha_0 \bar{i}'}{\varrho'\omega_k^2}\right) = 0 \tag{51}$$

to determine the angle α.

The coefficients in equation (51) are to be found as follows:

Acceleration $\bar{a}$ (through which according to (8) the pole distance p is determined), and the angular velocity ω_k can be considered as given values, and angle ξ can be determined according to (21) with the introduction of γ. In addition the value of $\bar{e}'$ can be determined from equation (20), and the magnitude ρ' from equation (35). In addition the tilting acceleration $\bar{i}'$ and the angle α_0 corresponding to the infinite pole distance should be computed.

Along with the designations of Figure 23 we have the following relations:

If the individual sides of triangle (S)KO are multiplied by ω_k^2, the sides of the vectorial triangle are produced, and in this sense

$$\bar{i}' = \overline{(S)O}\,\omega_2^k$$

and

$$(S)O = (S)T + TO = \sqrt{p^2 - \bar{e}'^2 \sin^2\xi} + \bar{e}'\cos\xi,$$

that is,

$$\bar{i}' = \omega_k^2 (\bar{e}'\cos\xi + \sqrt{p^2 - \bar{e}'^2\sin^2\xi}). \tag{52}$$

In order to determine the angle α_0 we make use of the right triangle KTB, the hypotenuse of which is

$$BK = \sqrt{\bar{e}'^2 + R_k^2 + 2\bar{e}' R_k \cos\xi} \approx \sqrt{R_k^2 + 2R_k \bar{i}'\cos\xi}$$

where

$$\cos\alpha = \frac{TK}{BK} = \frac{\bar{e}'\sin\xi}{\sqrt{R_k^2 + 2R_k\bar{e}'\cos\xi}}. \tag{53}$$

Knowing the angle of inclination α of the oblique lines allows the following magnitudes to be computed: from equations (48) or (49) the diameter of the Thales circle, the length of thrust amplitude y, the projection of the path y in the direction of acceleration $\bar{i}'$, and finally the thrust velocity.

The thrust amplitude reaches its greatest value with an infinite pole distance. This is produced from the right triangle OO_0J_0 under consideration of (53) /62

$$y = D_k \cos \alpha_0 = \frac{2 R_k \bar{c}' \sin \xi}{\sqrt{R_k^2 + 2R_k \bar{c}' \cos \xi}} = \frac{2\bar{c}' \cos \xi}{\sqrt{1 + \frac{2\bar{c}' \cos \xi}{R_k}}}. \tag{54}$$

Projection in the direction of the tilting force:

$$u = y_{\beta} \cos \alpha_0 = D_k \cos^2 \alpha_0. \tag{55}$$

According to point 2 of Section VI

$$i \approx \bar{a},$$

is valid for the case of a pole lying in infinity, and in consideration of (55) the final velocity amounts to:

$$v_2 = \sqrt{2iu} = \cos \alpha_0 \sqrt{2\bar{a} D_k}, \tag{56}$$

and the "fall time", i.e., the tilting time:

$$t = \sqrt{\frac{2D_k}{i'}} \approx \sqrt{\frac{2D_k}{\bar{a}}}. \tag{57}$$

4. The Greatest Dynamic Effect

In equations (50) and (51) we obtained useful quantitative expressions to characterize various operational cases, but it is simple to recognize the typical cases by geometric deduction from the Thales circle.

Figure 23 shows that the greatest value of the thrust amplitude y according to equation (54) is to be expected with the slowest rotational velocity (i.e., at zero revolutions).

From Figures 23 and 23a a circle can be determined from the various Thales circles where the projection of a path segment inclined by angle α_u on the force line of the tilting force is greatest, and where the maximum of final velocity is v_2. According to the picture this limiting case appears connected with the condition that the line connecting the end point of the vibration amplitude with midpoint K is parallel to the tilting force vector.

In such a case according to Figures 23a and 23b the coincidence of the triangles is: /63

$$\triangle CHO_u \simeq \triangle KT_u O_u ,$$

precisely because the segments

$$HO_u = TK = KT_u = \varrho'$$

are equal, and there is also uniformity of angles. Thus we obtain the radius of the Thales circle

$$CO - KO_u = R_T = \bar{e}'$$

and

$$u_{max} = \bar{e}' - \bar{e}' \cos \xi = \bar{e}'(1 - \cos \xi) . \tag{58}$$

To the diameter of the Thales circle

$$D_T = 2\bar{e}'$$

there belongs according to (48) the tilting velocity

$$\bar{i}' = \frac{\bar{e}' \omega_k^2}{(\alpha_0 - \alpha_u)^2} . \tag{59}$$

By dividing by ω_k^2 we get the side SO of the force triangle:

$$SO = \frac{\bar{i}'}{\omega_k^2} = \frac{\bar{e}'}{(\alpha_0 - \alpha_u)^2} .$$

Now from triangle SKO we get

$$SK = p_u = \frac{\bar{a}}{\omega_k^2} = \frac{\bar{a}}{\left(\frac{n\pi}{30}\right)^2 \left(\frac{d}{D+d}\right)^2} = \sqrt{\bar{e}'^2 + \frac{\bar{e}'^2}{(\alpha_0 - \alpha_u)^4} - 2\frac{\bar{e}'^2 \cos \xi}{(\alpha_0 - \alpha_u)^2}} , \tag{60}$$

and by means of equation (58) we get from the right triangle HOO_u

$$\tan\alpha_u = \frac{HO_u}{HO} = \frac{\varrho'}{u_{max}} = \frac{\bar{e}'\sin\xi}{\bar{e}'(1-\cos\xi)},$$

and

$$\tan\alpha_u = \frac{\sin\xi}{1-\cos\xi} = \frac{1}{\tan(\xi/2)}. \tag{61}$$

From the isosceles triangle OO_uC we get: /64

$$u_{max} = \bar{e}' - \sqrt{\bar{e}'^2 - \varrho'^2}, \tag{62}$$

and

$$u_{max} = \bar{e}'\left(1 - \sqrt{1-\left(\frac{\varrho'}{\bar{e}'}\right)^2}\right) = \bar{e}'(1 - \sqrt{1-\sin^2\xi} = \bar{e}'(1-\cos\xi).$$

In accord with the acceleration value according to equation (59) we here obtain the greatest thrust velocity:

$$v_{2max} = \sqrt{2\bar{i}'u_{max}} = \sqrt{\frac{2\bar{e}'\omega_k^2}{(\alpha_0-\alpha_u)^2}\bar{e}'(1-\cos\xi)},$$

and

$$v_{2max} = \frac{\bar{e}'\omega_k\sqrt{2(1-\cos\xi)}}{(\alpha_0-\alpha_u)} = \frac{2\bar{e}'\omega_k}{(\alpha_0-\alpha_u)}\sin\left(\frac{\xi}{2}\right). \tag{63}$$

In consideration of the initial conditions, the greater the pole distance, the more exact is the approximate computation with the aid of the Thales circle, and if this circle diameter approaches zero, this method of computation loses its significance.

XI. SLIPPING

1. With One Bearing Ball

In Chapter VII we have derived a method of computation by means of which the forces can be determined which affect the individual pairs of balls in one stable ball rim; this way of thinking helps us to be able to analyze in more detail both the circumstances of rolling and also the conditions of slipping.

In Figure 24 we see the shape of deformation of a single ball and of the rolling paths. As we see, load distribution on the deformation circle is not uniform, because the load is larger in the starting half and smaller in the ending half. By calling on the principle of similarity we can state that we get the spoke f of rolling friction if we always multiply the diameter θ of the elastic flattening by the same constant factor χ:

$$f = \chi\theta,$$

where the factor χ depends on the elasticity of the materials touching one another. If we presume a uniform load distribution along the flattening semicircle, χ with the spoke of the mass midpoint of the loaded semicircular arc is equal to /65

$$\chi = \frac{2\theta}{3\pi}.$$

But now the surface pressure is greater in the vicinity of the midpoint, and because we must deal with the unloading activity of the ending semicircle (depending on the elasticity of the materials), the inequality below is effectively valid

$$\chi < 0.2\theta.$$

In Videky [15] we find information about the friction coefficients of cylindrical surfaces; this equation was derived from the Hertzian equations and the pertinent geometric configurations, and is written as follows:

$$f = f_0 + 0{,}38\sqrt{\frac{P'}{E}\cdot\frac{1}{r_1+r_2}}\cdot\frac{r_1-r_2}{\sqrt{r_1 r_2}}.$$

Here f_0 is the coefficient of friction in the normal direction, and P' is the reduced pressure on the unit length (cm) of the cylinder length. This equation can be used without further ado for the case of roller bearings (with cylindrical or conical rollers). On the other hand, the presumption of direct proportionality of the friction of the bearing ball to the diameter of the flattening is sufficient for ball bearings.

We begin with the Hertzian equation [16] while maintaining the designations of Figure 24:

$$\vartheta = 2{,}22\sqrt[3]{\frac{N}{E}\frac{(b/2)\cdot r}{(b/2)+r}},$$

and

$$\vartheta' = 2{,}22 \sqrt[3]{\frac{N}{E} \cdot \frac{(b/2)R}{(b/2)+R}}$$

For the contact between two convex surfaces it should be:

$$r = (+\ k)\ \frac{b}{2}\ ;$$

and for contact between a convex and a concave surface:

$$R = (+\ k)\ \frac{b}{2}\ ,$$

and in consideration of the relationship /66

$$R_k = 2r + b = d + b = 2R - b = D - b,$$

$$\vartheta = 2{,}22 \sqrt[3]{\frac{N}{E}\frac{b}{2}\left(\frac{k}{1+k}\right)} = 1{,}76 \sqrt[3]{\frac{N}{E}\frac{bd}{R_k}} \tag{64}$$

and

$$\vartheta' = 2{,}22 \sqrt[3]{\frac{N}{E}\frac{b}{2}\left(\frac{K}{K-1}\right)} = 1{,}76 \sqrt[3]{\frac{N}{E}\frac{bD}{R_k}}; \tag{64a}$$

and for the lever arm of rolling friction

$$f = 1{,}76\,\varkappa \sqrt[3]{\frac{N}{E}\frac{bd}{R_k}} = C \sqrt[3]{\frac{Nbd}{R_k}}; \tag{65}$$

and

$$f' = 1{,}76\,\varkappa \sqrt[3]{\frac{N}{E}\frac{bD}{R_k}} = C \sqrt[3]{\frac{NbD}{R_k}} \tag{65a}$$

with the value

$$C = 2{,}22 \sqrt[3]{\frac{1}{2E}}$$

as material constants.

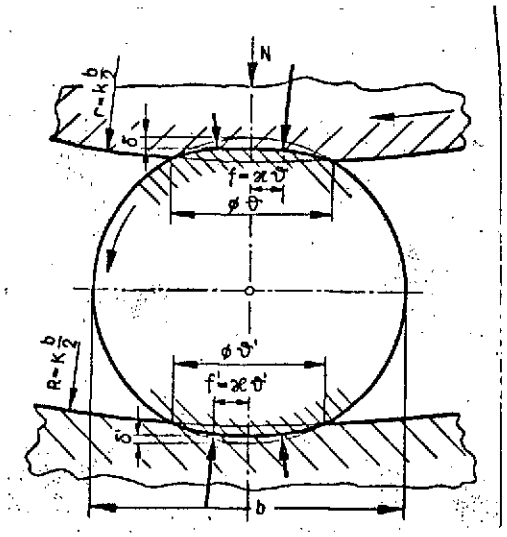

Figure 24. Deformation of the Ball and of the Roller Paths in the Case of a Single Ball.

Maintaining designations of Figure 25 and with μ as the coefficients of slipping friction, the frictional force operating on ball B according to equation (18) is

$$\mu N_1 = \mu \frac{N}{2 \cos \gamma} .$$

2. The Case With One Bearing Pair of Balls

/67

Our research is primarily valid for the condition of slipping in a pair of bearing balls (Figure 25).

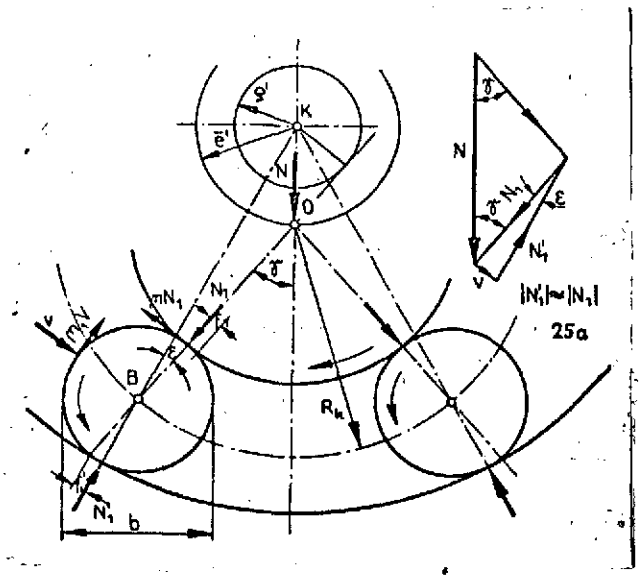

Figure 25. The Condition of Slipping In the Case Of Only One Pair Of Bearing Balls. a) Vector Diagram.

This force will only compel the ball to roll when the torque moment operating on the diametrially opposed point is greater than the moment which can be computed from the cage friction $(\mu_1 V)b/2$ and the roller resistance at the point mentioned, where μ_1 signifies the frictional coefficient valid here and the pertinent roller resistances affect the following arms:

$$f_1 = C \sqrt[3]{\frac{N_1 bd}{R_k}} = C \sqrt[3]{\frac{Nbd}{2 \cos \gamma R_k}}$$

and

$$f_1' = C \sqrt[3]{\frac{NbD}{2 \cos \gamma R_k}} .$$

The momentary equation is produced from the load of two balls of the pair of balls: /68

$$M = 2N_1 \mu b \geq 2N_1 f_1 + 2N_1 f_1' + 2V\mu_1 \frac{b}{2},$$

where (in accord with Figure 25a) the following relationships also exist:

$$V = N_1 \sin \varepsilon = N_1 \frac{\varrho'}{BK} = \frac{N_1 \bar{e}' \sin \gamma}{\sqrt{\bar{e}'^2 + R_k^2 + 2\bar{e}' R_k \cos \gamma}} \approx \frac{N_1 \bar{e}' \sin \gamma}{\sqrt{R_k^2 + 2\bar{e}' R_k \cos \gamma}},$$

i.e., in consideration of equations (18), (65) and (65a):

$$\frac{\mu N}{2 \cos \gamma} \geq \frac{N}{2 \cos \gamma} \frac{C}{b} \sqrt[3]{\frac{Nbd}{2 \cos \gamma R_k}} + \frac{N}{2 \cos \gamma} \frac{C}{b} \sqrt[3]{\frac{NbD}{2 \cos \gamma R_k}} + \frac{N\mu_1 \bar{e}' \sin \gamma}{2 \cos \gamma \sqrt{R_k^2 + 2\bar{e}' R_k \cos \gamma}},$$

i.e., rolling begins if the condition

$$\mu \geq \frac{C}{b} \sqrt[3]{\frac{Nb}{2 \cos \gamma R_k}} \left(\sqrt[3]{d} + \sqrt[3]{D}\right) + \frac{\bar{e}' \sin \gamma \mu_1}{R_k \sqrt{1 + \frac{2\bar{e}' \cos \gamma}{R_k}}} \qquad (66)$$

is fulfilled.

But if μ is smaller than this expression, slipping will occur.

3. The Case With Several Bearing Pairs of Balls

With several pairs of balls the rolling condition can be written as follows:

$$\mu(N_1 b + N_2 b + \ldots) \geq N_1(f_1 + f_1') + N_2(f_2 + f_2') + \ldots + \frac{N_1 \bar{e}' \sin \gamma \mu_1}{\sqrt{R_k^2 + 2R_k \bar{e}' \cos \gamma}} + \frac{N_2 \bar{e}' \sin 3\gamma \mu_1}{\sqrt{R_k^2 + 2R_k \bar{e}' \cos 3\gamma}} + \ldots,$$

where the corresponding N-values can be computed with equation (26) or from the table given. This tedious computation simply indicates the relationship that the limiting condition of slipping depends on the frictional values μ and μ_1, as well as on the elastic properties of the material, the construction properties of the roller bearings and the magnitude of the load.

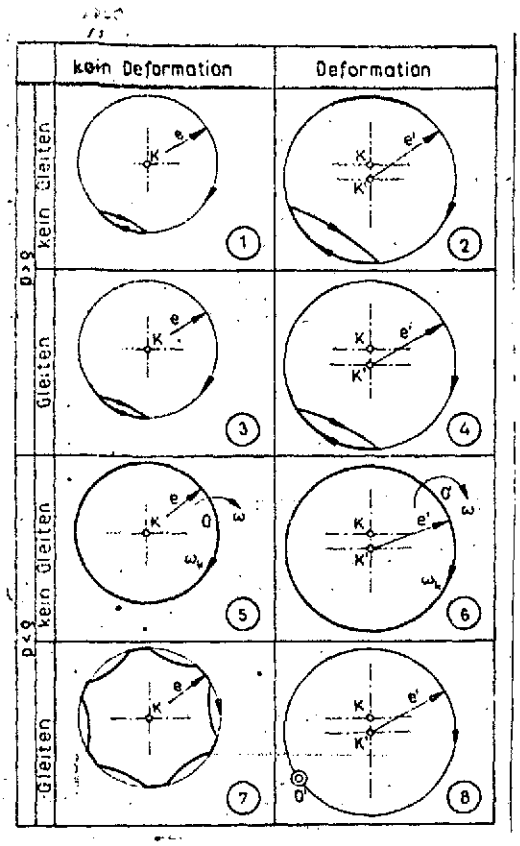

Figure 26. Various Varieties of Vibration Phenomena.

In consideration of the possibility of slipping we can define eight different variations of vibration phenomena, depending upon the occurrence or lack of deformation. These variations are summarized as in a table in Figure 26, naturally for a roller bearing with clearance and with the assumption of a rotating system balanced on its own axis. /69

4. The Vibration Phenomena For The Case Characterized by $p > \rho$ (Figure 26).

(1) Purely kinetic vibrations; characterized by the fact that only the bearing pairs of balls come in contact with each other;

(2) A magnitude of the half load angle fluctuates between γ and 180°; $\rho < \rho' < e'$;

(3) Rocking and tilting on a circle of radius e;

(4) Rocking and tilting on a circle of diameter e'.

5. Vibration Phenomena For The Case Characterized by $p < \rho$ /70

This case has only been mentioned in passing in the previous considerations; in our way of thinking we have not adduced any theoretically proven determinations; the variations presented here (in Figure 26) under 5...8 can be considered as probabilities until experiments have clarified the circle phenomena characterized by $p < \rho$.

(5) Planet movements; the shaft turns about on its own midline and executes a circular motion on a circle of radius e on the same pair of balls, and this lasts until the number of revolutions drops.

(6) Planet movement on several pairs of bearing balls on one curve of radius $e' > e$, but without friction of the carrying pairs of balls.

(7) Tilting movements during the circular movement caused by slipping.

(8) If the load arc is great enough, it is conceivable that the shaft "is shifted by a definite angle" in the direction of turn, and that during rotation the midline of the shaft continues in an unstable position (it is possible for the cage to rotate at half speed).

XII. THE EFFECT OF THE DEFORMATION VELOCITY

In our above exposition it was convenient for the sake of simplicity and uniformity to adopt a uniform course of tilting motion for all angular values ξ. But this variation is only possible under the assumption that the velocity of deformation remains behind the rate of change in the effective force. In reality the occurrence of a "sharp" tipping is to be considered as probable only with simultaneous operation of a few bearing balls, large bearing clearance, and a high rotation number.

If bearing clearance is small, load great and rotation number low, every ball involved in tilting has enough time available to flatten itself under the load even before the entire load sector has been covered. In such a case there can scarcely be any talk of the tipping of the entire load segment; a "coasting process" occurs here when the individual ball enters the load angle sector.

But we very well know the property of materials, namely that the more suddenly forces follow each other the more brittle they are. Consequently the greater the revolutions with the same clearance and unchanged load, the stronger the tilting.

REFERENCES

1. Stribeck, "Ball Bearings for Any Loads," *Z.V.D.I.*, No. 3, p. 73, No. 4, p. 118, 1901.
2. Jurgensmeyer, W., *Die Waelzlager* [The Roller Bearings], Verlag von Julius Springer, Berlin, 1937 (With an exhaustive list of specialized bibliography).
3. Perret, H., "Roller Bearings as Causes of Vibration," *Werkstattstechnik und Maschinenbau*, No. 1, p. 5, 1950.
4. Perret, H., "Elastic Clearance Vibrations of Constantly Loaded Roller Bearings," *Werkstatt und Betrieb*, p. 354, 1950.
5. Perret, H., "Axial Play and Radial Play of Ball Bearings," *Werkstatt und Betrieb*, No. 3, p. 91, 1950.
6. Perret, H., "Bearing Play as a Decisive Magnitude for Strain on a Roller Bearing," *Werkstatt und Betrieb*, p. 131, 1950.
7. Perret, H., "Vibrations in Roller Bearings With Statically Determined Reinforcement," *V. D. I. Forschungsheft*, 434, Edition B, Vol. 18, p. 17, 1952.
8. Meldau, E., "The Pressure Distribution in Play-Free Roller Bearings With Variable Pressure Angle," *V. D. I. Forschungsheft*, p. 421, 1943.
9. Meldau, E., "The Movement of the Axis of Roller Bearings at Small Revolutions," *Werkstatt und Betrieb*, No. 7, p. 308, 1951.
10. Szoke, B., "Vibrations Occurring During Turning," *Nepszava Konyvkiado*, Budapest, 1953.
11. Szoke, B., "Independent Action of Friction Bearings," *Gep*, No. 113, 1956.
12. Kihlberg, B., "Spindle Bearings in Abrasive and Cutting Machines," *SKF Kugellager Zeitschrift*, No. 27, 1955.
13. Kinberg, R., "Silent Bearings," *SKF Kugellager Zeitschrift*, No. 3, 1956.
14. Hungarian Standards MSZ 7980 and 7986. Roller Bearings. Norms for Bearing Clearance.
15. Videky, E., *Fogaskerekek I. Resz.* [Cogwheels, Part I], Patria Irodalmi Vallalat es Nyomdai Reszvenytarsasag, Budapest, 1911.
16. Hermann, M., *Gepelemek* [Machine Elements], Nemeth Jozsef Technikai Konyvkereskedese, Budapest, 1924.
17. ten Bosch, M., "Computation of Machine Elements," Berlin, 1951.
18. *SKF Kugellager Zeitschrift*, No. 2, pp. 32-34, 1949.
19. Muttnyanszky, A., *Statika II. Kiadas* [Statistics, Second Edition], Tankonyvkiado, Budapest, 1952.
20. Nagy, D., *Dinamika* [Dynamics], Magyar Mernok es Epitesz-Egylet, Budapest, 1905.
21. Voros, I., *Gepelemek* [Machine Elements], Muszaki Egyetemi Jegyzet, Budapest, 1952.
22. Banki, D., *Hidrogepek. Keziratos Jegyzet* [Hydraulic Machinery. Hand Written Notes], Budapest, 1920.
23. SKF Main Catalog of Roll and Ball Bearings, 5,400 items.
24. SKF Bearings in Machine Tools, (Reg. 872.0. 1744 n.e. Feb. 46).
25. Szoke, B., "The Possibility of Kinetic Vibration in Antifriction Bearings," *Acta Techn. Hung.*, No. 27, pp. 3-24.
26. Szoke, B., "Kinetic Vibrations in Roller Bearings," *Technische Rundschau* (Part 2, Machine Elements), Vol. 53, No. 28, pp. 9-13, Bern., 1961.

27. Szoke, B., "The Basic Phenomena of Ball Bearing Vibrations," *Maschinenbautechnik*, 10, No. 12, pp. 625-631, 1961.
28. Szoke, B., "Fundamental Phenomena of Kinetic Vibrations of Roller Bearings," *M. T. A. Muszaki Tud. Oszt. Kozlemenyei*, Vol. 30, pp. 341-364.

NOTE: References 25-28 refer to vibrations in roller bearings with rigid, rather than elastic, components.

Translated for the National Aeronautics and Space Administration under Contract No. NASw-2485 by Techtran Corporation, P. O. Box 729, Glen Burnie, Md. 21061.